



Lipidic synthetic alkaloids as SK3 channel modulators. Synthesis and biological evaluation of 2-substituted tetrahydropyridine derivatives with potential anti-metastatic activity

Sana Kouba, Julien Braire, Romain Félix, Aurélie Chantôme, Paul-Alain Jaffres, Jacques Lebreton, Didier Dubreuil, Muriel Pipelier, Xuexin Zhang, Mohamed Trebak, et al.

► To cite this version:

Sana Kouba, Julien Braire, Romain Félix, Aurélie Chantôme, Paul-Alain Jaffres, et al.. Lipidic synthetic alkaloids as SK3 channel modulators. Synthesis and biological evaluation of 2-substituted tetrahydropyridine derivatives with potential anti-metastatic activity. European Journal of Medicinal Chemistry, 2020, 186, pp.111854. 10.1016/j.ejmech.2019.111854 . hal-03027843

HAL Id: hal-03027843

<https://hal.science/hal-03027843>

Submitted on 6 Sep 2022

HAL is a multi-disciplinary open access archive for the deposit and dissemination of scientific research documents, whether they are published or not. The documents may come from teaching and research institutions in France or abroad, or from public or private research centers.

L'archive ouverte pluridisciplinaire **HAL**, est destinée au dépôt et à la diffusion de documents scientifiques de niveau recherche, publiés ou non, émanant des établissements d'enseignement et de recherche français ou étrangers, des laboratoires publics ou privés.

Lipidic alkaloids as SK3 channel modulators. Synthesis and biological evaluation of 2-substituted tetrahydropyridine derivatives with potential anti-metastatic activity.

Sana Kouba,^a Julien Braire,^b Romain Félix,^a Aurélie Chantôme,^a Paul-Alain Jaffrès,^c Jacques Lebreton,^b Didier Dubreuil,^b Muriel Pipelier,^b Xuexin Zhang,^d Mohamed Trebak,^d Christophe Vandier,^a Monique Mathé-Allainmat^{b*} and Marie Potier-Cartereau^{a*}

a) University of Tours, Inserm U1069 Nutrition, Croissance et Cancer (N2C), Faculty of Medicine, 10 boulevard Tonnellé 37032 Tours Cedex, France.

b) University of Nantes, CNRS, Faculty of Sciences, Chimie et Interdisciplinarité: Synthèse, Analyse, Modélisation (CEISAM), UMR CNRS 6230, 2, rue de la Houssinière, 44322 Nantes Cedex 3, France.

c) University of Brest, CNRS, CEMCA, UMR 6521, 6 Avenue Victor Le Gorgeu, 29238 Brest, France.

d) Pennsylvania State University College of Medicine, Department of Cellular and Molecular Physiology, 700 HMC Crescent Road, Hershey, PA 17033 USA.

*Both authors supervised equally the research work

Abstract

Small Conductance Calcium (Ca^{2+})-activated potassium (K^+) channels (SKCa) are now proved to be involved in many cancer cell behaviors such as proliferation or migration. The SK3 channel isoform was particularly described in breast cancer where it can be associated with the Orai1 Ca^{2+} channel to form a complex that regulates the Ca^{2+} homeostasis during tumor development and acts as a potent mediator of bone metastases development *in vivo*. Until now, very few specific blockers of Orai1 and/or SK3 have been developed as potential anti-metastatic compounds. In this study, we illustrated the synthesis of new families of lipophilic pyridine and tetrahydropyridine derivatives designed as potential modulators of SK3 channel. The toxicity of the newly synthesized compounds and their migration effects were evaluated on the breast cancer cell line MDA-MB-435s. Two molecules (**7a** and **10c**) demonstrated a significant decrease in the SK3 channel-dependent migration as well as the SK3/Orai1-related Ca^{2+} entry. Current measurements showed that these compounds are more likely SK3-selective. Taken all together these results suggest that such molecules could be considered as promising anti-metastatic drugs in breast cancer.

Keywords: Ca^{2+} -activated K^+ channels; SK3; breast cancer; cell migration; amphiphilic compounds; tetrahydropyridine derivatives.

1. Introduction

Calcium (Ca^{2+}) is a ubiquitous second messenger and its cytosolic concentration is highly regulated by a wide variety of Ca^{2+} pumps, channels and transporters.¹ In a physiological context, elevated concentrations of cytosolic Ca^{2+} are necessary to activate several types of ion channels of which, the Ca^{2+} -activated K^+ channels (KCa).² The increased K^+ permeability consequent to elevate cytosolic Ca^{2+} was initially illustrated in red blood cells more than 50 years ago and later then, pharmacological manipulation of cytosolic Ca^{2+} led to the identification of KCa channels in molluscan neurons.³ Consequently, a classification of the KCa channels was made according to their single channel conductance, molecular and pharmacological properties into three major subfamilies: the Big-conductance Ca^{2+} -dependent K^+ channels (BKCa channels), the Intermediate-conductance Ca^{2+} -dependent K^+ channels (IKCa channels), and the Small-conductance Ca^{2+} -dependent K^+ channels (SKCa channels). The SKCa channels have small single-channel conductance (10-20 pS) and are thus named “small-conductance” channels.⁴ Four genes encoding the SKCa channels have been identified: *KCNN1* for SK1 (also named KCa1.1), *KCNN2* for SK2 (also named KCa2.1), *KCNN3* for SK3 (also named KCa2.3) and *KCNN4* for SK4 (also named KCa3.1) with highly conserved sequences among species. Numerous studies focused on the roles of the SKCa channels which are widely expressed in excitable cells.⁵ Their functional disruptions have been associated to many neurological diseases such as Parkinson’s disease, bipolar disorder and schizophrenia.^{6,7,8} SKCa dysfunctions have also been associated to cardiovascular pathologies such as cardiac arrhythmia, atrial fibrillation and hypertension.^{9, 10, 11, 12} In addition to their implication in neurological and cardiovascular diseases in excitable cells, their role in non-excitabile cells such as epithelial cells was mostly described in cancer. The most compelling results highlighting an evident connection between the SKCa channels expression and cancer cell biology were mainly obtained from studies on breast cancer.¹³ A work from our laboratory has shown that the SK3 channel was abnormally expressed in the non-excitabile breast cancer cell line (MDA-MB-435s) and was found to promote cancer cell migration *in vitro* and bone metastasis formation *in vivo*.¹⁴ Chantôme *et al.*, demonstrated an association between the SK3 channel and the Orai1 Ca^{2+} channel in distinct nanodomains of the plasma membrane enriched with cholesterol and sphingolipids known as lipid rafts. In association with Orai1, the SK3 induced a hyperpolarization of the membrane leading to an increase of the Ca^{2+} electrochemical driving force and a constitutive Ca^{2+} entry *via* Orai1. This association between Orai1 and SK3 creates

a positive loop since the Ca^{2+} influx *via* Orai1 not only activates the Ca^{2+} -dependent migration of cancer cells, but it also increases the activity of the SK3 channel (see **Fig. S1** in SI).

In breast cancer, 60% of patients with advanced breast cancer will eventually develop bone metastases (BM) during the course of disease. One of the greatest challenges in breast cancer treatment is then to limit the formation of BMs and until now, no treatment to prevent this event has been proposed. The available therapies on the market are mainly to improve the life quality of patients by limiting the bone resorption and fractures.¹⁵ Because SK3 was found to be implicated in the migration of breast cancer cells and BMs development, it has become a challenge for scientists to identify novel compounds to modulate its migratory activity.

Several natural compounds extracted from scorpions, sea anemone or bee venom have already been described to act on SKCa channels.^{16,17,18} The most known compound is apamin, a neurotoxic peptide found in bee venom. Apamin efficiently blocks SKCa channels without having an effect on BKCa and IKCa channels.¹⁹ Despite its efficiency on SKCa channels, this molecule was not selective between the SKCa isoforms. Consequently, during the two last decades crystallographic²⁰ and molecular modelling²¹ studies have contributed to design and identify synthetic drugs as positive or negative modulators of the SKCa channels with specific sites of action. The anti-bacterial drug dequalinium chloride was shown to be a SKCa channel blocker at the apamin allosteric binding site.²² Synthetic analogues of dequalinium salt, with a constrained cyclic structure, such as ULC 1684, were identified to present activities at low nanomolar range (**Fig. 1**).²³ Extending this SAR study to bis-charged tetraazacyclophanes bearing an aliphatic bridging chain didn't give better result.²⁴ Complementary studies from a pharmacophore model based on apamin and UCL1684 structures resulted in the identification of bis-isoquinolinium derivatives²⁵ and tetrahydroisoquinolinium analogues such as NMAG525E1²⁶ as high affinity ligands for SK2/SK3 channel subtypes (**Fig. 1**).

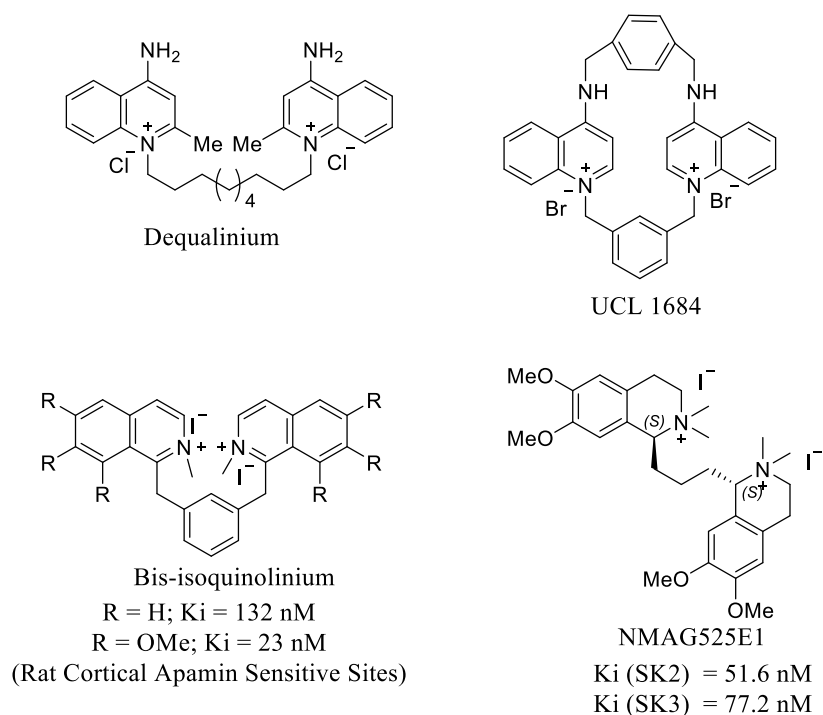


Fig. 1: Charged compounds identified as inhibitors of SK2/SK3 channels, targeting the Apamin binding site.

If these compounds bearing permanent charges could be regarded as apamin competitors, some small neutral molecules were also proved to act as negative or positive modulators of SKCa channels targeting both SK2 and SK3 types. As an example, the amino pyrimidine derivative CyPPA²⁷ or the amino naphthothiazol SKA-31 and analogues²⁸ were characterized as positive modulators of the gating system binding at the channel/calmoduline interface (**Fig. 2**). Whereas the *N*-alkyl-amino benzimidazole compound NS8593, with an additional tetrahydronaphthalene moiety, appeared to be a potent negative gating modulator, rather than a pore blocker. Further investigations on the mode of action of NS8593 have pointed out possible interactions of the molecule at position deep within the inner pore vestibule.²⁹

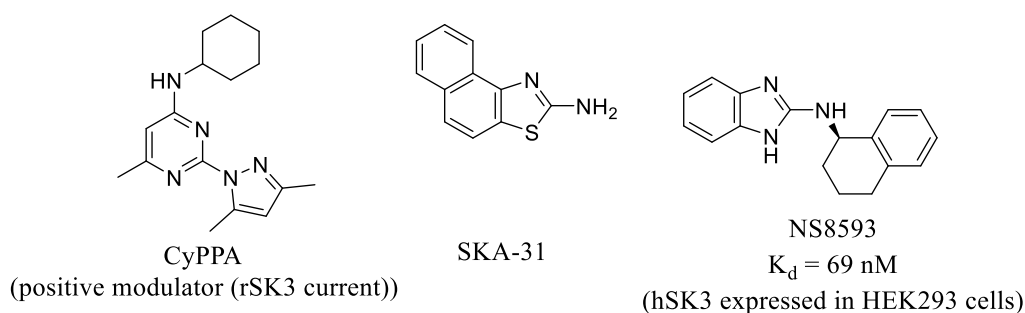


Fig 2: Neutral compounds as SK2/SK3 channels positive or negative modulators

As *supra* discussed, it is only recently that the involvement of SK3 in cancer cell behaviors such as cell proliferation or cell migration was highlighted. Consequently, charged phospholipidic molecule such as edelfosine (**Fig. 3**) was found to disrupt SK3 activity through a novel mechanism of action within the lipid rafts. This amphiphilic compound perturbed the association of SK3 and Orai1 at the plasma membrane to block cell migration.³⁰ However, its toxic effect at moderate concentration (3 μ M) allowed the chemists to design and synthesize sugar analogs such as neutral glyco-glycero-ether lipids among which, ohmline appeared as the most efficient member (**Fig. 3**).³¹ Ohmline inhibited selectively the SK3 current and activity by decreasing the migration of breast cancer cells *in vitro* at low concentrations (300 nM)³² and also reduced the development of BMs in a mouse model *in vivo* as shown by Chantôme *et al.*¹⁴

In this study we described the synthesis of a novel amphiphilic family of compounds bearing a pyridine or tetrahydropyridine moiety, as found in some apamin competitors, and a saturated or unsaturated fatty chain (**Fig. 3**, compounds **A** and **B**). The lipidic chain was introduced starting from selected saturated (C18, C20) or unsaturated (C18:1-cis- ω 9) fatty carboxaldehydes. A highly metastatic breast cancer cell line (MDA-MB-435s) expressing the SK3 channel (shRD cells) or not (shSK3 cells) was chosen in order to evaluate the toxicity of the novel compounds. The molecules with a poor or without toxicity up to 1 μ M were selected and their effects on the SK3-dependent migration, Ca^{2+} influx and current were investigated.

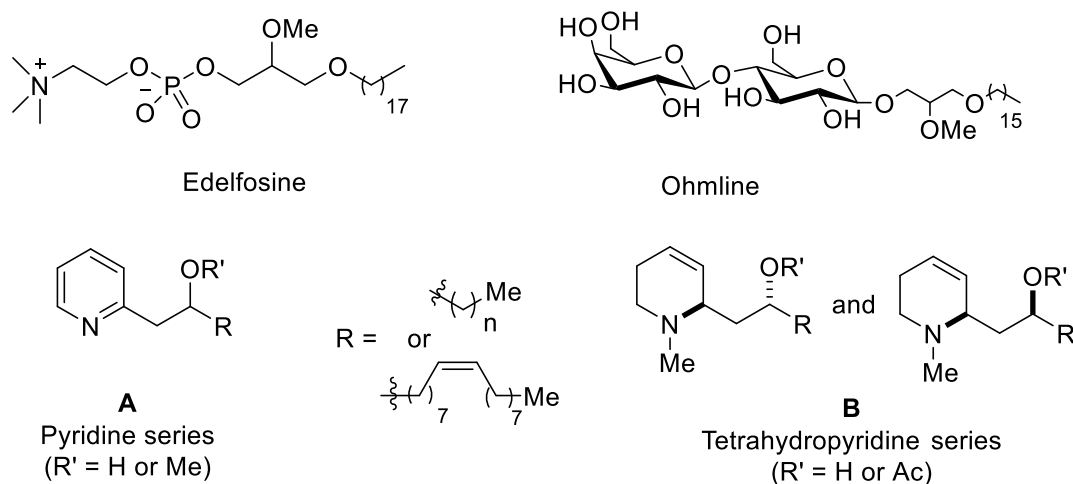
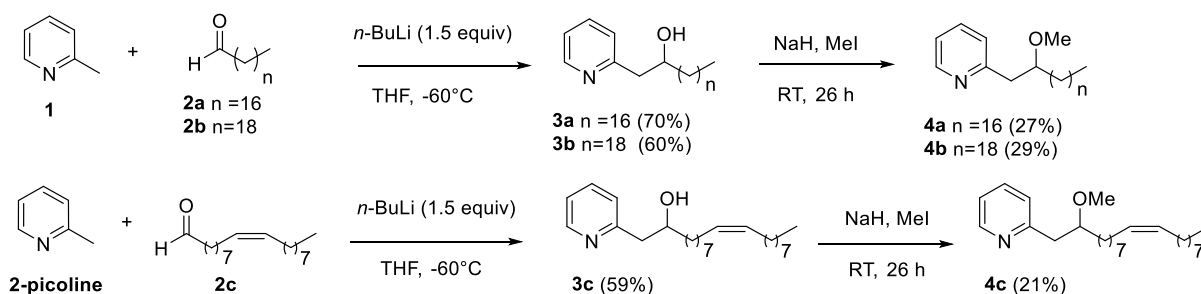


Fig.3: Edelfosine and ohmline as amphiphilic hSK3 blockers and novel pyridine and tetrahydropyridine targeted compounds **A** and **B**.

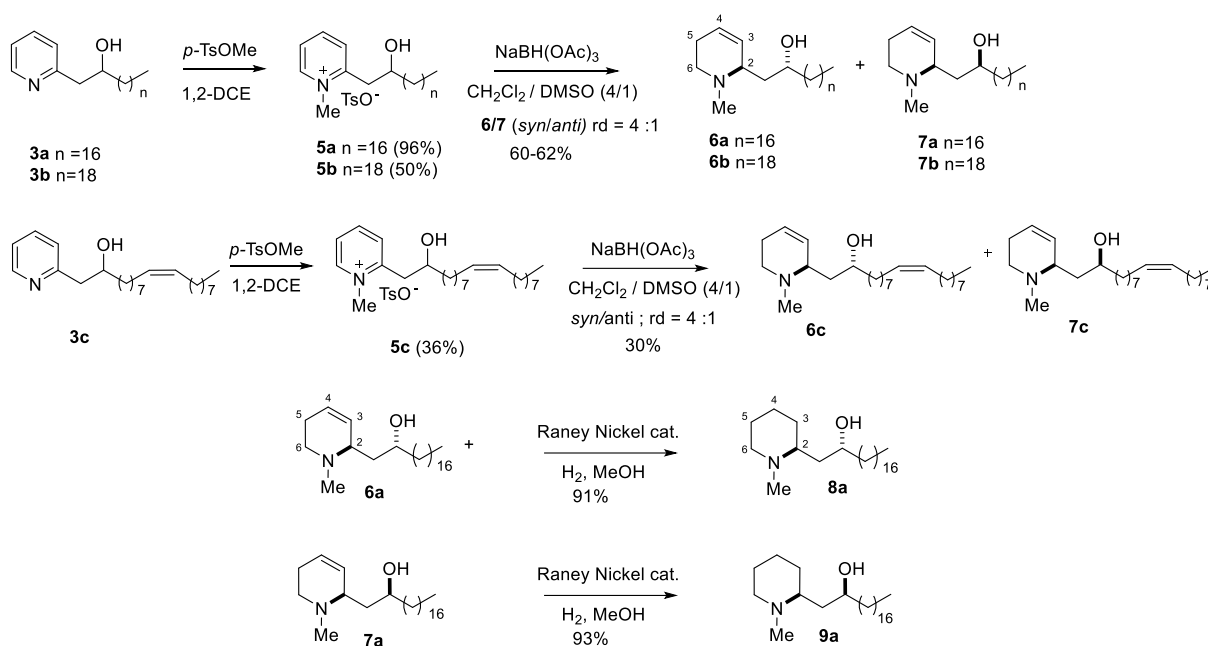
2. Results and discussion

2.1 Chemistry:

The novel amphiphilic compounds in series **A** and **B** were prepared following a short and simple strategy we earlier published³³ using commercially available 2-picoline **1**, and selected aldehydes **2a-c** prepared by oxidation of the corresponding alcohols (**Scheme 1**). The length of the lipophilic chain was fixed at 16 to 18 methylene carbons close to that found in ohmline and edelfosine compounds. The addition of the lithiated 2-picoline on the aldehydes **2a-c** at low temperature afforded the hydroxy compounds **3a-c** in 59-70% yields. These pyridine intermediates were quaternarized to their corresponding *N*-Me-pyridinium salts **5a-c** in the presence of methyl paratoluene sulfonate in refluxing dichloroethane. Moderate to good yields of compounds **5** were obtained after a simple filtration of the precipitate formed in the reaction medium (**5a**: 96 %; **5b**: 50 %; **5c**: 39 %). Some assays were carried out using methyl iodide as the *N*-alkylating agent but the purification procedure of the iodide salts by simple precipitation appeared less efficient. The pyridinium p-toluenesulfonate salts **5a-c** were reduced to *N*-Me-tetrahydropyran derivatives **6a-c** and **7a-c**, by treatment with an excess of sodium triacetoxyborohydride in a mixture of DMSO/CH₂Cl₂ (**Scheme 2**). In these conditions, the reduction of the pyridinium salts **5a-c** proceeded with the formation of the sole 3,4-tetrahydropyridine regioisomers and a good diastereoselectivity in favor of the *syn*-(±)-**6a-c** isomers over the *anti*-(±)-**7a-c** (4:1 ratio). Isomers **6a/7a** and **6b/7b** were formed in 60% and 62% yields respectively, whereas **6c/7c** were formed in a moderated 30% yield. Pure compounds **6** and **7** were isolated by chromatography purification to be evaluated. To confirm the structures of both diastereoisomers, *syn*-**6a** and *anti*-**7a** derivatives were hydrogenated in the presence of Raney Nickel to avoid double bond migration and consequently C2 epimerisation.³⁴ The corresponding *syn*-**8a** and *anti*-**9a** diastereoisomers were isolated in good yields (**Scheme 2**).

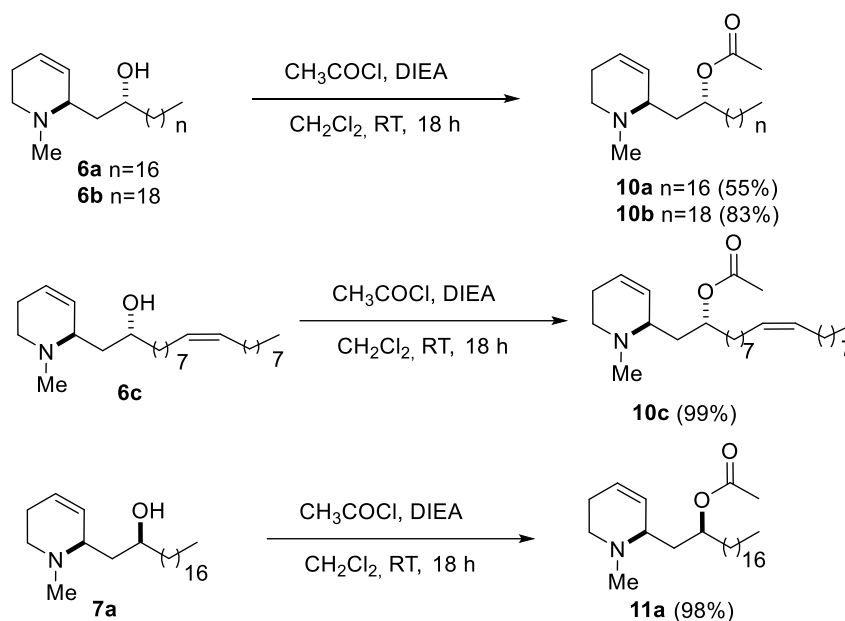


Scheme 1 : Synthesis of the pyridine derivatives **3a-c** and **4a-c**



Scheme 2: Synthesis of the tetrahydropyridine derivatives **6a-c** : **7a-c** and piperidine derivatives **8a** and **9a**.

Some modifications of the free hydroxyl group in compounds **3** and **6/7** were proposed. Indeed, *O*-methylation of the compounds **3a-c** was achieved using NaH as the base in the presence of an excess of MeI as alkylating agent (**Scheme 1**). The corresponding compounds **4a-c** were isolated after column chromatography purification with low yields (**4a**: 27%; **4b**: 29% and **4c**: 21%) due to the formation of byproducts such as quaternarized pyridine derivatives. Therefore, esterification of tetrahydropyridine compounds **6a-c** and **7a** was performed with acetyl chloride in the presence of diisopropylethylamine, leading to the corresponding acetates **10a-c** and **11a** in good to excellent yields (**10a** : 55 %; **10b** : 83 %, **10c** : 99 % and **11c** : 98 %) (**Scheme 3**).



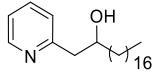
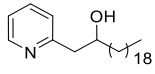
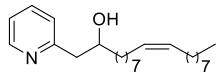
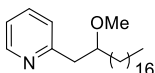
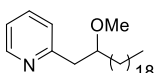
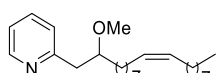
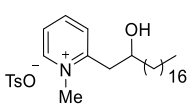
Scheme 3: Synthesis of the *O*-acetyl derivatives **10a-c** and **11a**

2.2 Biological results and discussion

2.2.1 Cytotoxicity evaluations

As a preliminary biological study, the cytotoxicity of the novel compounds **3a-c**, **4a-c**, **6a-c**, **7a-c**, **10a-c** and **11a** was evaluated to exclude toxic effects on cell proliferation. We therefore treated the MDA-MB-435s cells at different concentrations of selected analogues using ohmline as reference (**Table 1**). Molecules showing little or no toxic effect at 1 μM were tested up to a maximal concentration of 10 μM whereas molecules having a toxic effect at 1 μM were further tested at maximum of 3 μM . We observed that pyridine derivatives (compounds **3** and **4**) systematically showed a toxicity at 1 μM , except for compounds **3a** and **4a** which had no toxic effect up to 10 μM . It is also to be noticed that charged *N*-methylated compound such as compound **5a** was more toxic than its pyridine precursor **3a**, perhaps due to the sulfonate counter ion in this *N*-methyl pyridinium form.

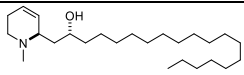
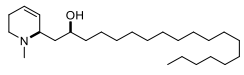
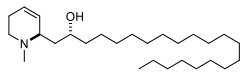
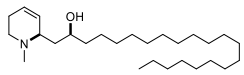
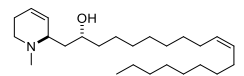
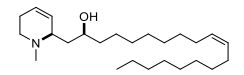
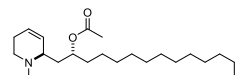
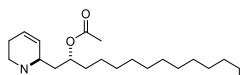
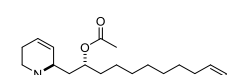
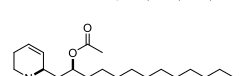
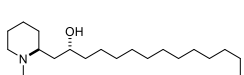
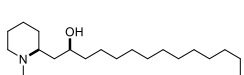
Table 1: Cytotoxic effects (24 hours treatment) of pyridine derivatives (**3a-c**, **4a-c** and **5a**) on MDA-MB-435s cancer cells compared to ohmline.

| Pyridine derivatives | | % of mortality | | |
|----------------------|---|----------------|-----------------|-----------------|
| | | 1 μ M | 3 μ M | 10 μ M |
| 3a |  | 0 | NT ^a | 0 |
| 3b |  | 20 | 20 | NT ^a |
| 3c |  | 20 | 25 | NT ^a |
| 4a |  | 0 | NT ^a | 0 |
| 4b |  | 20 | 20 | NT ^a |
| 4c |  | 20 | 25 | NT ^a |
| 5a |  | 30 | NT ^a | 80 |
| Ohmline | | 0 | 0 | 0 |

^a) NT for not tested

For the tetrahydropyridine compounds (**6**, **7**, **10** and **11**) or for piperidine analogues (**8a** and **9a**), the cytotoxicity seemed lower compared to the pyridine parents (**Table 1**) since most of them showed no effect at 1 μ M (**Table 2**). This behavior was systematically observed for all the compounds bearing the shorter lipophilic chain (**6a**, **7a**, **8a**, **9a**, **10a** and **11a**). For the compounds with a longer saturated or unsaturated carbon chain, the *O*-acylated form (**10b** and **10c**) also appeared less toxic than the parent compounds (**6b** and **6c**). Furthermore, the tetrahydropyridine compounds **6a-c**, **7a-c**, **10a-c** and **11a** were tested for their *in vitro* inhibition of cell proliferation on a panel of seven human tumor cell lines (Huh7, CaCo2, MDA-MB231, HCT116, PC3, NCI-H727 and MCF7) with the normal diploid skin fibroblasts used as a control (**Table 3**). All novel derivatives presented a very poor toxicity, with an IC₅₀ up to 6 μ M, particularly compounds **6a/7a** and **6b/7b** which have shown no effect up to 25 μ M on the seven cancer cell lines as well as on fibroblasts.

Table 2: Cytotoxic effects (24 hours treatment) of the tetrahydropyridine derivatives (**6a-c**, **7a-c**, **8a**, **9a**, **10a-c** and **11a**) and piperidine derivatives (**8a** and **9a**) on MDA-MB-435 cells (NT stands for not tested).

| Tetrahydropyridine and piperidine derivatives | | % of mortality | | |
|--|---|----------------|-----------------|-----------------|
| | | 1 μ M | 3 μ M | 10 μ M |
| 6a |  | 0 | NT ^a | 80 |
| 7a |  | 0 | NT ^a | 0 |
| 6b |  | 20 | 30 | NT ^a |
| 7b |  | 30 | 30 | NT ^a |
| 6c |  | 30 | 80 | NT ^a |
| 7c |  | 30 | 40 | NT ^a |
| 10a |  | 5 | NT ^a | 70 |
| 10b |  | 0 | NT ^a | 20 |
| 10c |  | 0 | NT ^a | 70 |
| 11a |  | 0 | NT ^a | 20 |
| 8a |  | 0 | NT ^a | 35 |
| 9a |  | 0 | NT ^a | 30 |
| Ohmline | | 0 | 0 | 0 |

^{a)} NT for not tested

Table 3: Antiproliferative activity of the tetrahydropyridine derivatives **6a-b**, **7a-b**, **10a-c** and **11a**.

| Compound | Cytotoxicity IC ₅₀ (μM) ^a | | | | | | | |
|--------------------|---|--------|------------|--------|------|----------|------|------------|
| | HuH7 | CaCo-2 | MDA-MB-231 | HCT116 | PC3 | NCI-H727 | MCF7 | Fibroblast |
| 6a | >25 | 21 | >25 | >25 | >25 | >25 | >25 | >25 |
| 6b | >25 | >25 | >25 | >25 | >25 | >25 | >25 | >25 |
| 6c | 10 | 8 | 8 | 10 | 7 | 9 | 10 | 9 |
| 7a | >25 | 16 | >25 | >25 | >25 | >25 | >25 | >25 |
| 7b | >25 | 14 | >25 | >25 | >25 | >25 | >25 | >25 |
| 7c | 24 | 6 | 14 | 15 | 19 | >25 | 18 | 25 |
| 10a | 22 | 9 | 21 | 16 | 15 | >25 | 19 | 18 |
| 10b | >25 | 17 | >25 | >25 | >25 | >25 | >25 | >25 |
| 10c | 10 | 9 | 10 | 9 | 8 | 19 | 15 | 13 |
| 11a | >25 | 9 | 22 | 24 | 26 | >25 | >25 | 24 |
| Doxorubicin | 0.03 | 0.17 | 0.02 | 0.12 | 0.12 | 0.66 | 0.16 | 0.03 |

^a) IC₅₀ was calculated after 48 h incubation with 6 concentrations of the compound (0.1 to 25 μM):

2.2.2. Modulation of SK3-dependent cell migration

After performing the viability tests, we proceeded on studying the effects of the molecules showing low or no toxicity, on the migration of MDA-MB-435s breast cancer cells at a single dose of 1 μM. Results showed that compounds **7a** and **10c** significantly decreased the migration of MDA-MB-435 cells up to 60 % and 40 % respectively (**Fig. 4**). In the same conditions Ohmlin (1 μM) decreased the migration of the cells around 35-40 %.

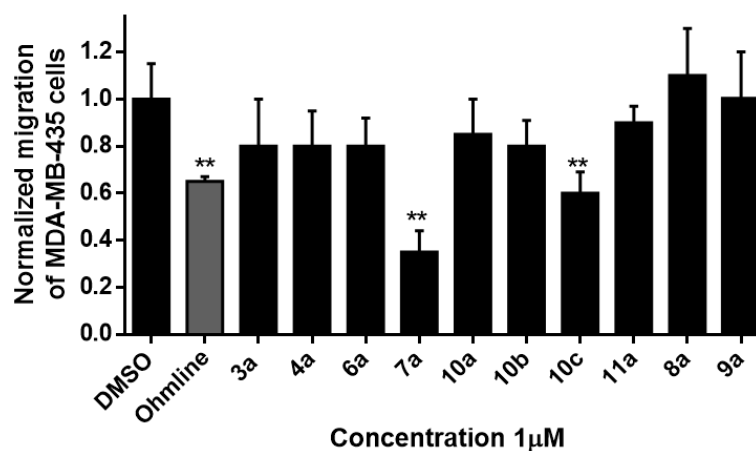


Fig. 4. Effect of the compounds at 1 μ M on the migration of MDA-MB-435s breast cancer cells. The normalized cell number corresponds to the ratio of the total number of migrating cells in the presence of the compounds/the total number of migrating cells in control experiments. Migration assays were realized for 24 hours in three separate experiments (in triplicate).

Based on these results, compound **7a** and its congener compound **10c** with structural modulations on the lipophilic residue, were selected for further biological evaluations. As a first approach, their inhibitory impact on the SK3-dependent migration was studied, followed by Ca^{2+} influx and currents measurements.

To determine if molecules **7a** and **10c** were SK3-selective, we generated cells lacking the expression of the SK3 channel (MDA-MB-435s shSK3). The experiments were performed and apamin was used as a positive control at a concentration of 100 nM (**Fig. 5**). At this concentration apamin is selective for SK3 and has no effect on SK1 or SK2. The molecule **7a** inhibited the migration of the MDA-MB-435s shRD cells up to 60 % at low concentrations (100 nM and 300 nM) (**Fig. 5A**) and did not affect the migration of MDA-MB-435 shSK3 cells (**Fig. 5B**). On the other hand, the molecule **10c** inhibited the migration of SK3-expressing cells in a dose dependent manner up to 40 % at 3 μ M (**Fig. 5C**) with no significant impact on the migration of the SK3-depleted MDA-MB-435 shSK3 cells (**Fig. 5D**). These data suggested that **7a** and **10c** were most likely SK3 selective. Furthermore, compound **7a** can be compared to the glyco-glycero lipid ohmlin identified previously as a SK3 blocker with around 40 % inhibition of MDA-MB-435s cell migration at 300 nM, and appeared to be as efficient as edelfosine C18 having 60% of potency at the same concentration.³¹

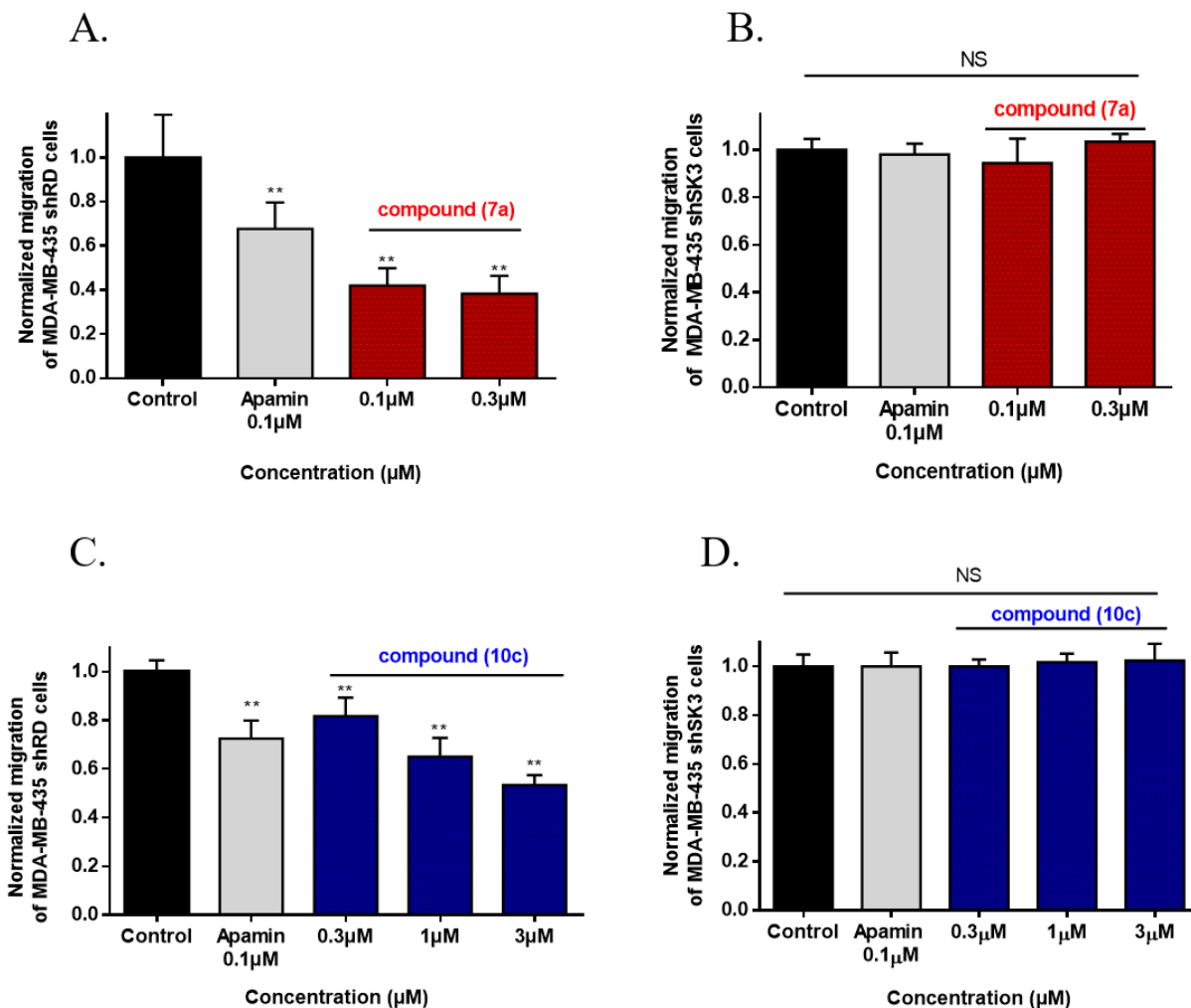


Fig. 5. Effect of **7a** and **10c** on the SK3-dependent migration of MDA-MB-435s breast cancer cells. **(A)** Dose-effect of compound **7a** on the MDA-MB-435s shRD cells expressing the SK3 channel. **(B)** Dose-effect of compound **7a** on MDA-MB-435s shSK3 cells **(C)** Dose-effect of compound **10c** on SK3-expressing cells and **(D)** Dose-effect of compound **10c** on MDA-MB-435s lacking the expression of SK3. Normalization corresponds to the ratio of the total number of migrating cells with the compounds / total number of migrating cells in control experiments. Migration assays were realized for 24 hours in three separate experiments (in triplicate). Histograms represent the mean \pm SEM.

2.2.3. *In vitro* effect on Ca^{2+} influx

In order to investigate whether the behaviors of **7a** and **10c** on the migration were SK3 and Ca^{2+} -dependent, we measured the constitutive Ca^{2+} entry in MDA-MB-435s shRD vs. MDA-MB-435s shSK3 transfected with a siRNA sequence directed against Orai1 (siOrai1) or not (siCTL) (note that, the experiments were performed 48 hours after the transfection). The

association between SK3 and the Ca^{2+} channel Orai1 at the plasma membrane of MDA-MB-435s, has already been described previously by our laboratory to induce a constitutive Ca^{2+} entry necessary for the migration and bone metastasis formation (see **Fig. S1**, SI).¹⁴ Consequently, one way to explain the observed inhibition of cancer cell migration is to measure the constitutive Ca^{2+} entry resulting from these channels association. After treating the cells for 1 hour with the compounds **7a** or **10c** at 300 nM and 1 μM respectively, cells were resuspended in a Ca^{2+} free solution for 20 seconds and the Ca^{2+} was added (2 mM solution). Compound **7a** inhibited the constitutive Ca^{2+} influx up to 40 % in MDA-MB-435s shRD expressing Orai1 (**Fig. 6B**) without any significant effect on the cells after Orai1 knock-down (**Fig. 6C**). In cells lacking the SK3 channel expression, the molecule **7a** has no effect on the constitutive Ca^{2+} influx in siCTL cells as well as in siOrai1 cells (**Fig. 6D** and **6E**). At a concentration of 1 μM , compound **10c** showed similar behaviors as **7a** (**Fig. 6A, 6B, 6C, 6D** and **6E**). These results suggest that both molecules **7a** and **10c** modulate the Ca^{2+} entry in MDA-MB-435s cells only in the presence of both SK3 and Orai1 meaning that they could potentially action the SK3/Orai1 channel complex.

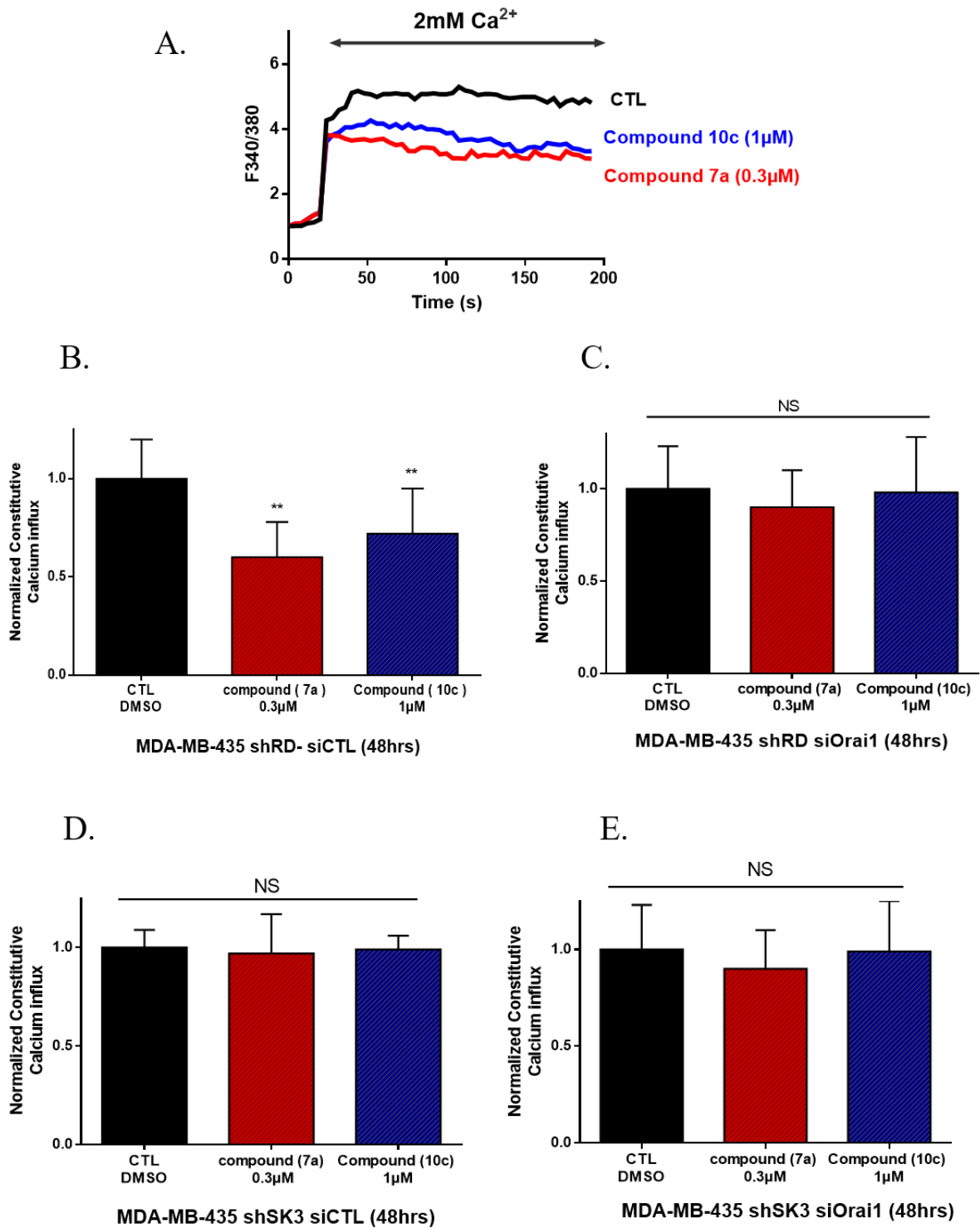


Fig. 6. Effect of **7a** and **10c** on the SK3-dependent constitutive Ca^{2+} entry in the MDA-MB-435s breast cancer cell line. **(A)** Graph showing steady state fluorescence relative to Ca^{2+} entry in the cells without and with 0.3 μM and 1 μM of **7a** and **10c** respectively. **(B)** Inhibition of the constitutive entry of Ca^{2+} with **7a** and **10c** in MDA-MB-435s shRD-siCTL cells. **(C)** Inhibition of the constitutive entry of Ca^{2+} with **7a** and **10c** in MDA-MB-435s shRD-siOrai1 cells. **(D)** and

(E) No significant effect of the molecules was detected under the same conditions on MDA-MB-435 shSK3. The results are obtained from three different experiments and each condition was performed in triplicate. Histograms represent the Mean \pm SEM of constitutive Ca²⁺ influx in presence of molecule normalized to control condition.

2.2.4. Effects on SK3 and CRAC currents

To follow the inhibitory role of compounds **7a** and **10c** on the SK3 current, the SK3 stable-expressing HEK-293 cells were used to measure the SK3 current with acute addition of **7a** (2 μ M) and **10c** (10 μ M) (**Fig. 7A**). Both molecules significantly inhibited the SK3 current but **7a** seemed to be more efficient with 90 % inhibition of the SK3 current (**Fig. 7B** and **7C**) compared to 70% for **10c** (**Fig. 7D** and **7E**). The 50 % inhibition of SK3 current occurred within approximately 10 seconds for **7a** compared to 100 seconds for **10c**. These results suggested that the compound **7a** was highly efficient. It is also to be noted that the addition of apamin induced an additive effect on the current inhibition. This result is of great interest because apamin is known to block the pore of the channel and the additive inhibitory effect induced by **7a** on the SK3 current suggests that this derivative might not be a pore blocker.

Because **7a** appeared to be a more potent modulator of SK3 current, we investigated whether **7a** acts on the CRAC current (Ca²⁺ Release Activated Ca²⁺ entry current or I_{CRAC}), generated by the Orai1 Ca²⁺ channel and its reticular regulator STIM1 (STromal interaction molecule1). Indeed, the Orai Ca²⁺ channel interacts with STIM1 and this interaction induces the Ca²⁺ entry *via* the Store Operated Ca²⁺ entry which is independent of the SK3 in our model of breast cancer. In order to investigate whether **7a** might act on Orai1 channel, I_{CRAC} was measured in stable Orai1/ STIM1- expressing HEK-293 cells. Acute application of **7a** (2 μ M) showed no effect on I_{CRAC} (**Fig. 8**) suggesting that **7a** is most likely specific to SK3 based on the massive inhibitory effect observed on the SK3 current.

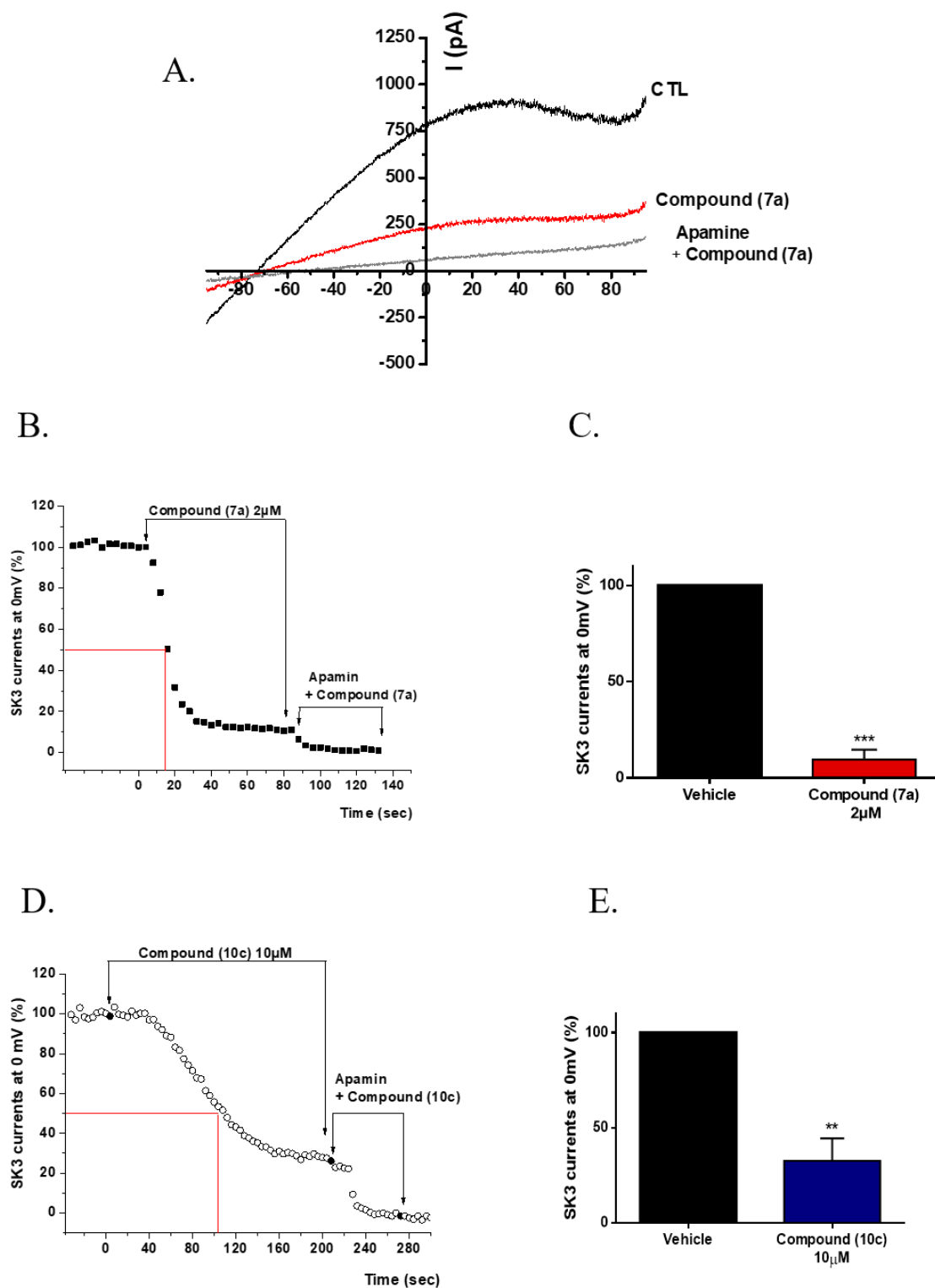


Fig. 7. Effect of **7a** and **10c** on the SK3 current in SK3 stable expressing HEK293 cells. **(A)** Representative current-voltage curves. The DMSO/Methanol mixture was used as vehicle control (in black). Acute addition of **7a** (2 μ M) with or without apamin (in gray and red respectively). **(B and C)** Time response inhibition of SK3 currents recorded at 0 mV with 2 μ M of **7a**. **(D and E)** Time response inhibition of the SK3 current recorded at 0 mV with 10 μ M of **10c**.

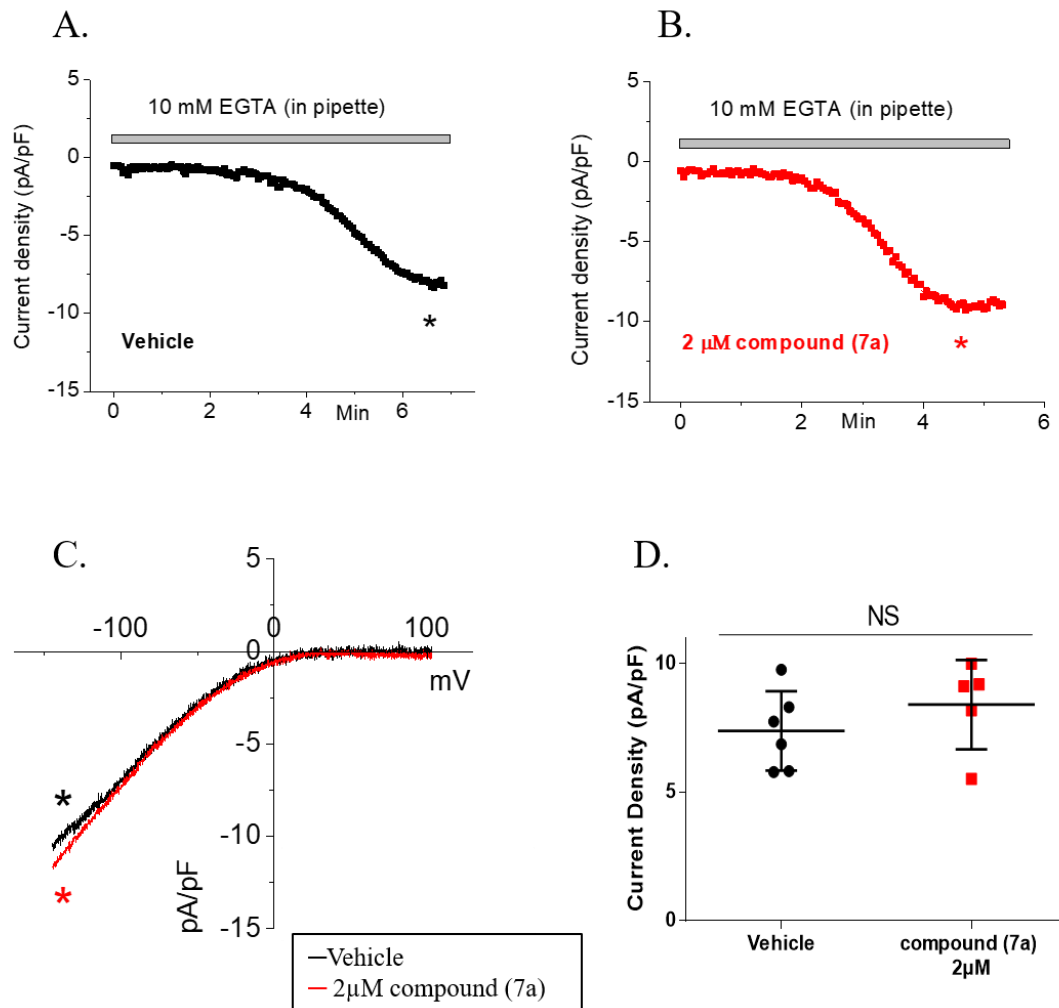


Fig. 8. The effect of **7a** on the Ca²⁺-Release Activated Current (CRAC current) in STIM1 and Orai1 stable expressing HEK293 cells. (**A** and **B**) Representative time-course traces of I_{crac} recorded from STIM1 and Orai1 stable expressing HEK293 cells. 10 mM EGTA was included in the patch pipette for store depletion. DMSO/Methanol was used as vehicle control in experiment (**A**) and 2 μM of **7a** was used in the bath for pre-incubation in experiment (**B**). (**C**) Representative current-voltage curves were taken from where indicated by the color-coded asterisks in A and B. (**D**) Quantification of current density for experiments **A** and **B**.

3. Conclusion

In this study we have prepared and evaluated novel series of pyridine and tetrahydropyridine compounds bearing a lipophilic chain and identified as new potential SK3 modulators. These molecules were efficiently prepared in three or four reaction steps starting from commercial 2-picoline and lipophilic aldehydes. Most of them revealed no intrinsic toxicity on a panel of cancer cell lines. The most efficient and promising compounds evaluated as cell migration blockers were obtained in tetrahydropyridine series. Among them, compound **7a** with a C17 saturated alkyl chain, and **10c** featuring a mono-unsaturated lipid chain were tested as potential SK3 channel modulators on MDA-MB-435s cells. The best compound **7a** gave efficient effect on breast cancer cell migration, with 60 % decrease of migration at 300 nM. This effect was shown to be greatly dependent of the presence of the SK3/Orai1 complex in the cells, but rather SK3 specific. Further complementary investigations are being carried out in our laboratory in order to establish the action mode of these compounds prior to run *in vivo* studies on xenograft mice models. The promising results observed in this study from *in vitro* experiments suggest that these two molecules **7a** and **10c** could be considered as a novel family of lipid compounds aiming to modulate ion channels' activity in cancer.

4. Experimental protocols

4.1 Chemistry

4.1.1 General experimental informations

All solvents used were reagent grade and TLC was performed on silica-covered aluminum sheets (Kieselgel 60F₂₅₄, MERCK). Eluted TLC was revealed using UV radiation ($\lambda = 254$ nm), or molybdate solution. Flash column chromatography was performed on silica gel 60 ACC 40-63 μ m (SDS-CarloErba). NMR spectra were recorded on a BRUKER AC300 (300 MHz for ¹H) or on a BRUKER 400 (400 MHz for ¹H) at room temperature, on samples dissolved in an appropriate deuterated solvent. References of tetramethylsilane (TMS) for ¹H and deuterated solvent signal for ¹³C were used. Chemical displacement values (δ) are expressed in parts per million (ppm), and coupling constants (*J*) in Hertz (Hz). Low-resolution mass spectra (MS) were recorded in the CEISAM laboratory on a Thermo-Finnigan DSQII quadripolar at 70 eV (CI with NH₃ gas). High-Resolution Mass Spectrometry (HRMS in Da unit) analyses were recorded on Xevo G2-XS Qtof apparatus (from Waters) in the laboratory, or on a MALDI - TOF-TOF apparatus (Autoflex III from Bruker) in the INRA center (BIBS platform, Nantes).

4.1.2. General synthetic procedure 1 for the synthesis of the aldehydes (2).

To a solution of the alcohol (1 equiv) in anhydrous DCM was added (diacetoxyiodo)benzene (1.1 equiv) followed by a catalytic amount of TEMPO (0.05 equiv) and the mixture was stirred during 18 h. The reaction was hydrolyzed with a saturated aqueous Na₂S₂O₃ solution and the compound was extracted with CH₂Cl₂. The organic layer was washed with a saturated aqueous NaHCO₃ solution then with brine, dried over MgSO₄, filtered and the solvent was removed under reduced pressure. Purification of the residue by column chromatography on silica gel (PE/CH₂Cl₂; 8:2) gave the expected pure aldehyde.

4.1.2.1. Octadecanal (2a): Following general procedure 1 and starting from commercial 1-octadecanol (15 g, 55 mmol), purification by column chromatography on silica gel afforded aldehyde **2a** as a white powder (83 % yield). ¹H NMR (300 MHz, CDCl₃): δ 9.75 (t, *J* = 1.8 Hz, 1H, CHO), 2.42 (dt, *J* = 7.2, 1.8 Hz, 2H, CH₂), 1.62 (quint, *J* = 7.2 Hz, 2H, CH₂), 1.25 (m, 28H, 14 x CH₂), 0.87 (t, *J* = 6.6 Hz, 3H, CH₃). ¹³C NMR (75 MHz, CDCl₃): δ 203.2 (CO), 44.2 (CH₂CO), 32.3-22.4 (14 x CH₂), 22.4 (CH₂), 14.3 (CH₃). MS (ESI) *m/z* 269.5 [M+H]⁺.

4.1.2.2. Eicosanal (2b): Following general procedure 1 and starting from commercial 1-eicosanol (5 g, 16.75 mmol) purification by column chromatography on silica gel afforded aldehyde **2b** as a white powder (77 % yield). ¹H NMR (300 MHz, CDCl₃): δ 9.76 (t, *J* = 1.8 Hz, 1H, CHO), 2.42 (dt, *J* = 7.2, 1.8 Hz, 2H, COCH₂), 1.62 (quint, *J* = 7.2 Hz, 2H, CH₂), 1.24 (m, 32H, 16 x CH₂), 0.87 (t, *J* = 7.1 Hz, 3H, CH₃). ¹³C NMR (75 MHz, CDCl₃): δ 203.1 (CO), 44.0 (CH₂CO), 32.07-29.83-29.57-29.50-29.31-28.83 (16 x CH₂), 22.23 (CH₂), 14.26 (CH₃). HRMS (ESI): calcd for C₂₀H₄₀ONa [M+Na]⁺ 319.2971, found 319.2970.

4.1.2.3. Cis-9-octadecenal (2c): Following general procedure 1 and starting from commercial oleyl alcohol (6.31 g, 20 mmol) purification by column chromatography on silica gel afforded aldehyde **2c** as a colourless oil (77 % yield). ¹H NMR (300MHz, CDCl₃): δ 9.76 (t, *J* = 1.8 Hz, 1H, CHO), 5.41-5.28 (m, 2H, CH=CH), 2.42 (dt, *J* = 7.2, 1.8 Hz, 2H, CH₂), 2.08-1.91 (m, 4H, 2 x CH₂), 1.61 (quint, *J* = 7.2 Hz, 2H, CH₂), 1.38-1.20 (m, 20H, 10 x CH₂), 0.87 (t, *J* = 6.6 Hz, 3H, CH₃). ¹³C NMR (75 MHz, CDCl₃): δ 202.81 (CO), 130.12 (CH=CH), 129.75 (CH=CH), 44.00 (COCH₂), 32.00 (2 x CH₂), 29.86-29.75-29.62-29.53-29.43-29.35-29.23-29.14-28.99-27.30 (10 x CH₂), 22.78 (CH₂), 22.16 (CH₂), 14.19 (CH₃). HRMS (ESI) calcd for C₁₈H₃₄ONa [M+Na]⁺ 289.2502, found 289.2506.

4.1.3. General synthetic procedure 2 for the synthesis of the pyridine derivatives (3).

To a solution of commercial 2-picoline (1.5 equiv) in anhydrous THF cooled to -70°C was slowly added *n*-BuLi (2.5 M solution in hexane, 1.5 equiv). The mixture was stirred at this temperature for 30 minutes and a solution of the aldehyde **2** in anhydrous THF (1equiv) was added dropwise to the red mixture at -60 °C. The reaction was stirred at this temperature during 3 h and then hydrolyzed with a saturated aqueous NH₄Cl solution. The compound was extracted with Et₂O. The organic layer was washed with a saturated aqueous NaHCO₃ solution then with

brine, dried over MgSO_4 , filtered and the solvent was removed under reduced pressure. Purification of the residue by column chromatography on silica gel ($\text{DCM}/\text{Et}_2\text{O}$: 8/2) gave the expected compound **3**.

4.1.3.1. 1-(pyridin-2-yl)nonadecan-2-ol (3a): Following the general procedure 2 and starting from octadecanal **2a** (1.67 g, 5.5 mmol), after purification, the expected compound **3a** was obtained as a white solid (70 % yield). ^1H NMR (300 MHz, CDCl_3): δ 8.49 (d, J = 4.8 Hz, 1H, CH_{ar}), 7.61 (dt, J = 7.7, 1.8 Hz, 1H, CH_{ar}), 7.17-7.12 (m, 2H, 2 x CH_{ar}), 4.03 (m, 1H, CHOH), 2.95-2.78 (m, 2H, CH_2), 1.56-1.24 (m, 32H, 16 x CH_2), 0.87 (t, J = 6.3 Hz, 3H, CH_3). ^{13}C NMR (75 MHz, CDCl_3): δ 160.14 (C_{ar}), 148.02 (C_{ar}), 137.21 (C_{ar}), 123.95 (C_{ar}), 121.60 (C_{ar}), 71.02 (CH), 43.09 (CH_2), 37.19 (CH_2), 31.91-29.69-25.66-22.68 (15 x CH_2), 14.11 (CH_3). HRMS (ESI) calcd for $\text{C}_{24}\text{H}_{44}\text{NO}$ [$\text{M}+\text{H}^+$] 362.3423, found 362.3426.

4.1.3.2. 1-(pyridin-2-yl)henicosan-2-ol (3b): Following the general procedure 2 and starting from eicosanal **2b** (1.67 g, 5.5 mmol), after purification, the expected compound **3b** was obtained as a white solid (yield 60 %). ^1H NMR (300 MHz, CDCl_3): δ 8.48 (d, J = 4. Hz, 1H, CH_{ar}), 7.61 (dt, J = 7.7, 1.8 Hz, 1H, CH_{ar}), 7.18-7.11 (m, 2H, 2 x CH_{ar}), 4.03 (m, 1H, CHOH), 2.95 (m, 2H, CH_2), 1.63-1.25 (m, 34H, 17 x CH_2), 0.88 (t, J = 6.3 Hz, 3H, CH_3). ^{13}C NMR (75 MHz, CDCl_3): δ 160.62 (C_{ar}), 148.75 (C_{ar}), 136.85 (C_{ar}), 123.83 (C_{ar}), 121.60 (C_{ar}), 71.18 (CH), 43.42 (CH_2), 37.32 (CH_2), 32.08-29.89-29.51-25.82-22.84- (17 x CH_2), 14.28 (CH_3). HRMS (ESI) calcd for $\text{C}_{26}\text{H}_{49}\text{NO}$ [$\text{M}+\text{H}^+$] 390.3736, found 390.3718.

4.1.3.3. (Z)-1-(pyridin-2-yl)nonadec-10-en-2-ol (3c) : Following the general procedure 2 and starting from aldehyde **2c** (3.5 g, 13.2 mmol), after purification, the expected compound **3b** was obtained as a colorless oil (59 % yield). ^1H NMR (300 MHz, CDCl_3): δ 8.47 (d, J = 4.8 Hz, 1H, CH_{ar}), 7.58 (dt, J = 7.7, 1.8 Hz, 1H, CH_{ar}), 7.14-7.10 (m, 2H, 2 x CH_{ar}), 5.34-5.27 (m, 2H, $\text{CH}=\text{CH}$), 5.07 (s, 1H, OH), 4.03 (m, 1H, CHOH), 2.93-2.27 (m, 2H, CH_2), 2.00 (m, 4H, 2 x CH_2), 1.60-1.25 (m, 24H, 12 x CH_2), 0.86 (t, J = 6.3 Hz, 3H, CH_3). ^{13}C NMR (75 MHz, CDCl_3): δ 160.5039 (C_{ar}), 148.51 (C_{ar}), 136.59 (C_{ar}), 129.83-129.78 ($\text{CH}=\text{CH}$), 123.61 (C_{ar}), 121.35 (C_{ar}), 70.91 (CH), 43.31 (CH_2), 37.11 (CH_2), 32.54 (CH_2), 31.84 (CH_2), 29.71-29.62-29.47-29.26-29.21-29.12-29.06-27.14-25.61-22.62 (11 x CH_2), 14.24 (CH_3). HRMS (ESI) calcd for $\text{C}_{24}\text{H}_{42}\text{NO}$ [$\text{M}+\text{H}^+$] 360.3266, found 360.3272.

4.1.4. General synthetic procedure 3 for the synthesis of the pyridine methoxy derivatives (**4**).

To a solution of the alcohol **3** (1 equiv) in THF (10 mL), was added sodium hydride (60 % dispersion in mineral oil, 1.5 equiv) at 0 °C. Methyl iodide (1.5 equiv) was introduced and the reaction was stirred during 28 h. Water was added and the product extracted with DCM. The organic layer was washed with brine, dried over MgSO_4 and concentrated under reduced pressure. The crude product was purified by flash column chromatography on silica gel ($\text{DCM}/\text{Et}_2\text{O}$:7/3) to give the expected product **4**.

4.1.4.1. 2-(2-methoxynonadecyl)pyridine (**4a**) : Following the general procedure 3 and starting from the alcohol **3a** (510 mg, 1.38 mmol), after purification, the expected compound **4a** was obtained as white powder (27 % yield). ¹H NMR (300 MHz, CDCl₃): δ 8.50 (m, 1H, CH_{ar}), 7.54 (td, *J* = 7.6, 1.8 Hz, 1H, CH_{ar}), 7.17 (d, *J* = 7.7 Hz, 1H, CH_{ar}), 7.07 (ddd, *J* = 7.4, 4.9, 0.9 Hz, 1H, CH_{ar}), 3.59 (quint, *J* = 5.3 Hz, 1H, CHOMe), 3.24 (s, 3H, OMe), 2.96 (dd, *J* = 13.5, 6.9 Hz, 1H, A part of ABX system CHH'), 2.86 (dd, *J* = 13.5, 5.7 Hz, 1H, B part of ABX system CHH'), 1.50- 1.22 (m, 32H, 16 x CH₂), 0.85 (t, *J* = 6.3 Hz, 3H, CH₃). ¹³C NMR (75 MHz, CDCl₃): δ 159.50 (C_{ar}), 149.11 (C_{ar}), 136.02 (C_{ar}), 124.06 (C_{ar}), 121.05 (C_{ar}), 81.10 (CHOMe), 56.94 (OMe), 42.89 (CH₂), 33.84 (CH₂), 31.86 (CH₂), 29.64- 29.53-29.30 (12 x (CH₂), 25.18 (CH₂), 22.62 (CH₂), 14.05 (CH₃). HRMS (ESI) calcd for C₂₅H₄₆NO, [M+H]⁺ 376.3574, found 376. 3575.

4.1.4.2. 2-(2-methoxyhenicosyl)pyridine (**4b**) : Following the general procedure 3 and starting from the alcohol **3b** (206 mg, 0.52 mmol), after purification, the expected compound **4b** was obtained as a white powder (29 % yield). ¹H NMR (300 MHz, CDCl₃): δ 8.53 (d, *J* = 4.4 Hz, 1H, CH_{ar}), 7.58 (td, *J* = 7.6, 1.8 Hz, 1H, CH_{ar}), 7.18 (d, *J* = 7.7 Hz, 1H, CH_{ar}), 7.11 (dd, *J* = 6.7, 5.1 Hz, 1H, CH_{ar}), 3.62 (quint, *J* = 6 Hz, 1H, CHOMe), 3.27 (s, 3H, OMe), 2.99 (dd, *J* = 13.6, 6.9 Hz, 1H, A part of ABX system CHH'), 2.86 (dd, *J* = 13.6, 5.7 Hz, 1H, B part of ABX system CHH'), 1.47- 1.25 (m, 36H, 18 x CH₂), 0.88 (t, *J* = 6.4 Hz, 3H, CH₃). ¹³C NMR (75 MHz, CDCl₃): δ 159.58 (C_{ar}), 149.11 (C_{ar}), 136.26 (C_{ar}), 124.13 (C_{ar}), 121.14 (C_{ar}), 81.18 (CHOMe), 57.04 (OMe), 42.97 (CH₂), 33.91 (CH₂), 31.91 (CH₂), 29.75- 29.69- 29.59 (14 x (CH₂), 25.25 (CH₂), 22.68 (CH₂), 14.11 (CH₃). HRMS (ESI) calcd for C₂₇H₅₀NO [M+H]⁺ 404.3892; found: 404.3878.

4.1.4.3. (Z)-2-(2-methoxynonadec-10-en-1-yl)pyridine (**4c**): Following the general procedure 3 and starting from the alcohol **3c** (250 mg, 0.56 mmol), after purification, the expected compound **4c** was obtained as an oil (21 % yield). ¹H NMR (300 MHz, CDCl₃): δ 8.52 (dd, *J* = 4.8, 0.8 Hz, 1H, CH_{ar}), 7.57 (td, *J* = 7.7, 1.8 Hz, 1H, CH_{ar}), 7.17 (d, *J* = 7.8 Hz, 1H, CH_{ar}), 7.10 (ddd, *J* = 7.3, 4.9, 0.8 Hz, 1H, CH_{ar}), 5.28- 5.36 (m, 2H, CH=CH), 3.61 (quint, *J* = 6 Hz, 1H, CHOMe), 3.27 (s, 3H, OMe), 3.99 (dd, *J* = 13.5, 7.0 Hz, 1H, A part of ABX system CHH'), 2.85 (dd, *J* = 13.5, 5.9 Hz, 1H, B part of ABX system CHH'), 2.0- 1.96 (m, 4H, 2 x CH₂), 1.51- 1.44 (m, 2H, CH₂), 1.37- 1.25 (m, 22H, 11 x CH₂), 0.86 (t, *J* = 6.4 Hz, 3H, CH₃). ¹³C NMR (75 MHz, CDCl₃): δ 160.04 (C_{ar}), 149.62 (C_{ar}), 136.46 (C_{ar}), 130.21-130.14 (CH=CH), 124.40 (C_{ar}), 121.39 (C_{ar}), 81.17 (CHOMe), 56.89 (OMe), 42.72 (CH₂), 33.62 (CH₂), 29.44- 29.33-29.19- 29.17-28.99-28.92 (9 x CH₂), 26.87 (2 CH₂), 24.90 (CH₂), 22.31 (CH₂), 13.69 (CH₃). HRMS (ESI) calcd for C₂₅H₄₄NO, [M+H]⁺ 374.3423, found 374.3432.

4.1.5. General synthetic procedure 4 for the synthesis of the tetrahydropyridine derivatives (**6**) and (**7**).

Methyl *p*-toluenesulfonate (1.5equiv) was added to a solution of the pyridine derivative **3** (1equiv) in dry 1,2-dichloroethane (150 mL). The mixture was refluxing during 18 h and a precipitate felt down which was filtered and washed with petroleum ether to afford pyridinium derivative **5**, used without further purification. The pyridinium salt **5** (1equiv) was then

dissolved in a mixture of DCM/DMSO (4: 1) and NaBH(OAc)₃ (2.5 equiv) were added. The reaction was stirred at room temperature for 2 days and then hydrolyzed with a saturated aqueous solution of NH₄Cl. The compound was extracted with DCM. The organic layer was washed with saturated aqueous NaHCO₃ then brine, dried (MgSO₄), filtered and the solvent was removed under reduced pressure. Purification of the residue by column chromatography on alumina gel (DCM/MeOH; 99.8:0.2) gave the expected pure diastereoisomers (±)-**6** and (±)-**7** as a racemic mixture.

4.1.5.1 (R)-1-((R)-1-methyl-1,2,5,6-tetrahydropyridin-2-yl)nonadecan-2-ol (6a) and (S)-1-((R)-1-methyl-1,2,5,6-tetrahydropyridin-2-yl)nonadecan-2-ol (7a) : Following the general procedure 4 and starting from the alcohol **3a** (5.2 g, 14.4 mmol), pyridinium derivative **5a** was obtained as a white powder (96 % yield). ¹H NMR (300 MHz, MeOD): δ 8.82 (d, *J* = 5.8 Hz, 1H, CH_{ar}), 8.46 (t, *J* = 7.1 Hz, 1H, CH_{ar}), 8.03 (d, *J* = 7.5 Hz, 1H, CH_{ar}), 7.88 (t, *J* = 7.1 Hz, 1H, CH_{ar}), 7.69 (d, *J* = 8.0 Hz, 2H, CH_{ar}), 7.23 (d, *J* = 8.0 Hz, 2H, CH_{ar}), 4.39 (s, 3H, NMe), 3.99 (m, 1H, CHOH), 3.28-3.14 (m, 2H, CH₂), 2.37 (s, 3H, CH₃Ph), 1.1.72-1.23 (m, 32H, 16 x CH₂), 0.90 (t, *J* = 6.3 Hz, 3H, CH₃). HRMS (ESI) calcd for C₂₅H₄₆NO, [M-Tos]⁺ 376.3579, found = 376.3582.

The pyridinium salt **5a** (2 g, 3.65 mmol) was reduced with NaBH(OAc)₃ to give after purification both isomers **6a** and **7a** (global yield : 62%). Pure fractions of each diastereoisomer could be obtained as an orange powder (**6a** 43 % yield; **7a** 5 % yield).

(6a) : ¹H NMR (300 MHz, CDCl₃): δ 5.79 (m, 1H, CH=CH), 5.54 (dq, *J* = 10.5, 1.2 Hz, 1H, CH=CH), 3.76 (quint, *J* = 6.6 Hz, 1H, CHOH), 3.09 (m, 2H, NCH and A part of ABX systems NCHH'), 2.65 (dd, *J* = 13.8, 5.7 Hz, 1H, B part of ABXX' system NCHH'), 2.47 (s, 3H, NMe), 2.24 (m, 1H, A part of ABXX' systems CH₂CHH'), 1.79 (dt, *J* = 17.7, 4.8 Hz, 1H, B part of ABXX' systems CH₂CHH'), 1.49-1.24 (m, 304H, 17 x CH₂), 0.88 (t, *J* = 6.3 Hz, 3H, CH₃). ¹³C NMR (75 MHz, CDCl₃): δ 127.83 (CH=CH), 124.74 (CH=CH), 72.81 (CHOH), 61.06 (NCH), 43.63 (NCH₂), 40.83 (NMe), 38.61 (CH₂), 38.23 (CH₂), 31.92 (CH₂), 29.78-29.69-29.36 (12 x CH₂), 25.47 (CH₂), 22.69 (CH₂), 18.53 (CH₂), 14.12 (CH₃). HRMS (ESI) calcd for C₂₅H₅₀NO, [M+H]⁺ 380.3892, found 380.3886.

(7a) : ¹H NMR (300 MHz, CDCl₃): δ 5.898 (m, 1H, CH=CH), 5.423 (m, 1H, CH=CH), 3.85 (m, 1H, CHOH), 3.04 (ls, 1H, NCH), 2.86 (m, 1H, A part of ABX systems NCHH'), 2.46 (s, 3H, NMe), 2.33 (m, 2H, B part of ABXX' system NCHH' and A part of ABXX' systems CH₂CHH'), 2.00- 1.86 (m, 2H, B part of ABXX' systems CH₂CHH' and A part of ABXX' systems CH₂CHH'), 1.47-1.24 (m, 32H, 2 x B part of ABXX' systems CH₂CHH' and 15 x CH₂), 0.87 (t, *J* = 6.3 Hz, 3H, CH₃). ¹³C NMR (75 MHz, CDCl₃): δ 128.57 (CH=CH), 126.47 (CH=CH), 69.28 (CH₂OH), 61.75 (CHN), 52.11 (CH₂N), 43.46 (NMe), 37.86 (CH₂), 36.39 (CH₂), 32.91 (CH₂), 29.812-29.68-28.60-29.34 (12 x CH₂), 25.63 (CH₂), 25.36 (CH₂), 22.67 (CH₂), 14.09 (CH₃). HRMS (ESI) calcd for C₂₅H₅₀NO, [M+H]⁺ 380.3892, found 380.3900.

4.1.5.2 (R)-1-((R)-1-methyl-1,2,5,6-tetrahydropyridin-2-yl)henicosan-2-ol (6b) and (S)-1-((R)-1-methyl-1,2,5,6-tetrahydropyridin-2-yl)henicosan-2-ol (7b) : Following the general procedure 4 and starting from the alcohol **3b** (1.45 g, 3.72 mmol), pyridinium derivative **5b** was obtained as a white powder (50 % yield). ¹H NMR (300 MHz, CDCl₃) δ 8.93 (d, *J* = 5.8 Hz, 1H, CH_{ar}),

8.22 (t, $J = 7.1$ Hz, 1H, CH_{ar}), 7.84 (d, $J = 7.5$ Hz, 1H, CH_{ar}), 7.74 (t, $J = 7.1$ Hz, 1H, CH_{ar}), 7.64 (d, $J = 8.0$ Hz, 2H, CH_{ar}), 7.1 (d, $J = 7.8$ Hz, 2H, CH_{ar}), 5.10 (sl, 1H, OH), 4.48 (s, 3H, NMe), 4.08 (m, 1H, CHOH), 3.14 (m, 2H, CH₂), 2.31 (s, 3H, CH₃Ph), 1.93-0.98 (m, 36H, 18 x CH₂), 0.87 (t, $J = 6.3$ Hz, 3H, CH₃). The pyridinium salt **5b** (1.37 g, 2.2 mmol) was reduced with NaBH(OAc)₃ to give after purification both isomers **6b** and **7b** (global yield : 62%). Pure fractions of each diastereoisomer could be obtained as a colored powder (**6b** 23 % yield; **7b** 4 % yield).

(6b) : ¹H NMR (300 MHz, CDCl₃): δ 5.76 (m, 1H, CH=CH), 5.53 (m, 1H, CH=CH), 3.77 (quint, $J = 6.6$ Hz, 1H, CHOH), 3.09 (m, 1H, A part of ABXX' system NCHH'), 3.03 (m, 1H, NCH), 2.61 (dd, $J = 13.8, 5.7$ Hz, 1H, B part of ABXX' system NCHH'), 2.45 (s, 3H, NMe), 2.23 (m, 1H, A part of ABXX' system CH₂CHH'), 1.76 (dt, $J = 17.7, 4.8$ Hz, 1H, B part of ABXX' systems CH₂CHH'), 1.47 (m, 4H, 2 x CH₂), 1.24 (m, 34H, 17 x CH₂), 0.86 (t, $J = 6.3$ Hz, 3H, CH₃). ¹³C NMR (75 MHz, CDCl₃): δ 128.34 (CH=CH), 125.08 (CH=CH), 73.26 (CHOH), 61.44 (NCH), 43.84 (NCH₂), 41.30 (NMe), 38.95 (CH₂), 38.58 (CH₂), 32.25 (CH₂), 30.12-29.62 (14 x CH₂), 25.80 (CH₂), 23.01 (CH₂), 18.85 (CH₂), 14.44 (CH₃). HRMS (ESI) calcd for C₂₇H₅₄NO, [M+H]⁺ 408.4200, found 408.4195.

(7b): ¹H NMR (300 MHz, CDCl₃): δ 5.88 (m, 1H, CH=CH), 5.42 (dt, $J = 9.9$ Hz, 1H, CH=CH), 3.86 (m, 1H, CHOH), 3.11 (m, 1H, NCH), 2.89 (m, 1H, A part of ABXX' system NCHH'), 2.42 (s, 3H, NMe), 2.36 (m, 2H, B part of ABXX' system NCHH' and A part of ABXX' system CH₂CHH'), 2.02 -1.85 (m, 2H, B part of ABXX' system CH₂CHH' and A part of ABXX' system CH₂CHH'), 1.42-1.24 (m, 35H, B part of ABXX' system CH₂CHH' and 17 x CH₂), 0.87 (t, $J = 6.3$ Hz, 3H, CH₃). ¹³C NMR (75 MHz, CDCl₃): δ 128.41 (CH=CH), 126.50 (CH=CH), 69.16 (CHOH), 61.62 (NCH), 52.01 (NCH₂), 41.35 (NMe), 37.98 (CH₂), 36.69 (CH₂), 32.05 (CH₂), 29.94-29.82-29.48 (14 x CH₂), 25.77 (CH₂), 25.06 (CH₂), 22.81 (CH₂), 14.24 (CH₃). HRMS (ESI) calcd for C₂₇H₅₄NO, [M+H]⁺ 408.4200; found 408.4202.

4.1.5.3 (R,Z)-1-((R)-1-methyl-1,2,5,6-tetrahydropyridin-2-yl)nonadec-10-en-2-ol (6c) and (S,Z)-1-((R)-1-methyl-1,2,5,6-tetrahydropyridin-2-yl)nonadec-10-en-2-ol (7c): Following the general procedure 4 and starting from the alcohol **3c** (2.9 g, 8.1 mmol), pyridinium derivative **5c** was obtained as a white powder (yield 36 %). ¹H NMR (300 MHz, DMSO-d₆): δ 8.95 (d, $J = 5.8$ Hz, 1H, CH_{ar}), 8.47 (t, $J = 7.8$ Hz, 1H, CH_{ar}), 8.03 (d, $J = 7.8$ Hz, 1H, CH_{ar}), 7.93 (t, $J = 6.4$ Hz, 1H, CH_{ar}), 7.47 (d, $J = 7.8$ Hz, 2H, 2 x CH_{ar}), 7.1 (d, $J = 7.8$ Hz, 2H, 2 x CH_{ar}), 5.33 (m, 2H, CH=CH), 5.02 (d, 1H, OH), 4.31 (s, 3H, NMe), 3.85 (m, 1H, CHOH), 3.36-3.03 (m, 2H, CH₂), 2.28 (s, 3H, CH₃Ph), 2.98 (m, 4H, 2 x CH₂), 1.52-1.25 (m, 24H, 12 x CH₂), 0.84 (t, $J = 6.3$ Hz, 3H, CH₃). HRMS (ESI) calcd for C₂₅H₄₄NO, [M-Tos]⁺ 374.3423, found 374.3426.

The pyridinium salt **5c** (1.2 g, 2.38 mmol) was reduced with NaBH(OAc)₃ to give after purification both isomers **6c** and **7c** (global yield : 30%). Pure fractions of each diastereoisomer could be obtained as a colored powder (**6c** 12 % yield; **7c** 2 % yield).

(6c) : ¹H NMR (300 MHz, CDCl₃): δ 5.74 (m, 1H, CH=CH), 5.53 (dq, $J = 10.5$ Hz, 1.2 Hz, 1H, CH=CH), 5.31 (m, 2H, CH=CH), 3.76 (quint, $J = 6.6$ Hz, 1H, CHOH), 3.10-3.02 (m, 2H, NCH and NCHH'), 2.62 (dd, $J = 13.8, 5.7$ Hz, 1H, NCHH'), 2.45 (s, 3H, NMe), 2.22 (m, 1H, A part of ABXX' system CH₂CHH'), 1.97 (m, 4H, 2 x CH₂), 1.75 (dt, $J = 17.7, 4.8$ Hz, 1H, B part of ABXX' system CH₂CHH'), 1.47 (m, 4H, 2 x CH₂), 1.24 (m, 22H, 11 x CH₂), 0.85 (t, J

= 6.3 Hz, 3H, CH₃). ¹³C NMR (75 MHz, CDCl₃): δ 130.89 (CH=CH), 130.17 (CH=CH), 128.18 (CH=CH), 125.03 (CH=CH), 73.11 (CHOH), 61.35 (NCH), 43.91 (NCH₂), 41.19 (NMe), 38.92 (CH₂), 38.53 (CH₂), 32.90 (CH₂), 32.20 (CH₂), 30.07-29.95-29.86-29.82-29.61- (8 x CH₂), 27.50 (CH₂), 25.76 (CH₂), 22.97 (CH₂), 18.85 (CH₂), 14.40 (CH₃). HRMS (ESI) calcd for C₂₅H₄₈NO, [M+H]⁺ 378.3730; found 378.3723.

(**7c**) : ¹H NMR (300 MHz, CDCl₃): δ 5.86 (m, 1H, CH=CH), 5.40 (d, *J* = 9.9 Hz, 1H, CH=CH), 5.32 (m, 2H, CH=CH), 3.85 (m, 1H, CHOH), 2.89 (m, 1H, NCH), 2.42 (s, 3H, NMe), 2.37 (m, 2H, NCH₂), 1.98-1.87 (m, 5H, 2 x CH₂ and A part of ABXX' system CH₂CHH'), 1.42-1.24 (m, 35H, B part of ABXX' system CH₂CHH' and 17 x CH₂), 0.86 (t, *J* = 6.3 Hz, 3H, CH₃). ¹³C NMR (75 MHz, CDCl₃): δ 130.33-129.87-126.6529 (2 x CH=CH), 68.79 (CHOH), 61.58 (NCH), 51.69 (NCH₂), 43.14 (low resolution NMe), 37.83 (CH₂), 36.68 (CH₂), 32.59 (CH₂), 31.88 (CH₂), 29.76-29.64-29.53-29.50-29.30-29.25-29.16-29.10 (9 x CH₂), 27.19 (CH₂), 25.59 (CH₂), 22.66 (CH₂), 14.45 (CH₃). HRMS (ESI) calcd for C₂₅H₄₈NO, [M+H]⁺ 378.3730, found 378.3726.

4.1.6. General synthetic procedure 5 for the synthesis of piperidine derivatives (**8a**) and (**9a**).

Compounds **6** or **7** (0.4 mmol) in solution in MeOH (5 mL) were hydrogenated under an atmosphere of H₂ in the presence of a catalytic amount of Raney Nickel (50% slurry solution in water). After 22 hours stirring at room temperature, the mixture was filtered and the solvent evaporated *in vacuo* to afford the expected pure piperidine compounds **8** or **9**.

4.1.6.1 (*R*)-1-((*S*)-1-methylpiperidin-2-yl)nonadecan-2-ol (**8a**). The tetrahydropyridine **6a** (0.16 g, 0.42 mmol) was hydrogenated following the general procedure 5, to give pure piperidine compound **8a** after simple filtration (93 % yield). ¹H NMR (300 MHz, CDCl₃): δ 3.76 (m, 1H, CHOH), 3.00 (m, 1H, A part of ABXX' system MeNCHH'), 2.66 (m, 1H, MeNH), 2.51 (m, 1H, B part of ABXX' system MeNCHH'), 2.42 (s, 3H, NMe), 1.87 (sex, 1H, A part of ABX systems CH(OH)CHH'), 1.69-1.24 (m, 37H, A part of ABXX' systems CH₂CHH', 17 x CH₂ and 2 x CH'H), 0.87 (t, *J* = 6.3 Hz, 3H, CH₃). ¹³C NMR (75 MHz, CDCl₃): δ 72.22 (CHOH), 60.86 (MeNCH), 51.58 (MeNCH₂), 39.93 (NMe), 38.45 (CH₂), 37.36 (CH₂), 31.91 (CH₂), 29.75-29.68-29.35 (12 x CH₂), 26.04 (CH₂), 25.57 (CH₂), 22.67 (CH₂), 22.57 (CH₂), 20.69 (CH₂), 14.10 (CH₃). HRMS (ESI) calcd for C₂₅H₅₂NO, [M+H]⁺ 382.4049, found 382.4062.

4.1.6.2 (*S*)-1-((*S*)-1-methylpiperidin-2-yl)nonadecan-2-ol (**9a**). The tetrahydropyridine **7a** (0.05 g, 0.13 mmol) was hydrogenated following the general procedure 5, to give pure piperidine compound **9a** after simple filtration (91 % yield). ¹H NMR (300 MHz, CDCl₃): δ 4.00 (m, 1H, CHOH), 2.88 (m, 1H, A part of ABXX' system MeNCHH'), 2.32 (s, 3H, NMe) 2.17 (m, 1H, MeNH), 1.94 (m, 2H, B part of ABXX' systems MeNCHH' and A part of ABX systems CH(OH)CHH'), 1.75 (m, 2H, 2 x CHH'), 1.57-1.20 (m, 37H, 17 x CH₂ and 3 x CHH'), 0.87 (t, *J* = 6.3 Hz, 3H, CH₃). ¹³C NMR (75 MHz, CDCl₃): δ 69.16 (CHOH), 62.92 (MeNCH), 57.42 (MeNCH₂), 44.09 (NMe), 38.20 (CH₂), 36.90 (CH₂), 31.91 (CH₂), 29.81-29.68-29.35 (13 x CH₂), 25.85 (CH₂), 25.65 (CH₂), 24.51 (CH₂), 22.67 (CH₂), 14.10 (CH₃). HRMS (ESI) calcd for C₂₅H₅₂NO, [M+H]⁺ 382.4049, found 382.4051.

4.1.7. General synthetic procedure 6 for the synthesis of the *O*-acetyl compounds (**10a-c**) and (**11a**).

To a solution of tetrahydropyridine derivative (**6** or **7**) (1equiv) in dry DCM (5mL), acetyl chloride (1.5eq) was added dropwise at 0°C followed by the addition of diisopropylamine (1.5 equiv). The solution was kept at 0°C for 1 h then stirred at room temperature overnight. It was hydrolyzed with a saturated aqueous NaHCO₃ solution, and the compound was extracted with DCM. The organic layer was washed with brine, dried (MgSO₄), filtered and the solvent was removed under reduced pressure. Purification of the residue by column chromatography on alumina gel (DCM/MeOH; 99.5:0.5) gave the expected compounds **10** or **11**.

4.1.7.1 (*R*)-1-((*R*)-1-methyl-1,2,5,6-tetrahydropyridin-2-yl)nonadecan-2-yl acetate (**10a**).

Following the general procedure 6 and starting from tetrahydropyridine derivative **6a** (100 mg, 0.26 mmol), compound **10a** was obtained as a brown oil (55 % yield). ¹H NMR (300 MHz, CDCl₃): δ 5.75 (m, 1H, CH=CH), 5.65 (m, 1H, CH=CH), 5.04 (m, 1H, CHOH), 2.47-2.38 (m, 1H, A part of ABX systems NCHH'), 2.64 (m, 1H, NCH), 2.38 (m, 1H, B part of ABXX' system NCHH'), 2.36 (s, 3H, NMe), 2.17 (m, 1H, A part of ABXX' systems CH₂CHH'), 2.00 (s, 3H, COCH₃), 1.95 (m, 2H, B part of ABXX' systems CH₂CHH' and A part of ABXX' systems CH(OH)CHH'), 1.63-1.50 (m, 3H, B part of ABXX' systems CH(OH)CHH') and CH₂), 1.23 (m, 30H, 15 x CH₂), 0.87 (t, *J* = 6.0 Hz, 3H, CH₃). ¹³C NMR (75 MHz, CDCl₃): δ 170.79 (CO), 128.46 (CH=CH), 125.04 (CH=CH), 71.34 (CHOH), 58.58 (NCH), 50.79 (NCH₂), 42.94 (NMe), 37.69 (CH₂), 35.20 (CH₂), 31.91-29.68-29.54-29.49-29.35 (15 x CH₂), 25.18 (CH₂), 21.27 (COCH₃), 14.11 (CH₃). HRMS (ESI) calcd for C₂₇H₅₂NO₂, [M+H]⁺ 422.3998, found 422.4005.

4.1.7.2 (*R*)-1-((*R*)-1-methyl-1,2,5,6-tetrahydropyridin-2-yl)henicosan-2-yl acetate (**10b**).

Following the general procedure 6 and starting from tetrahydropyridine derivative **6b** (122 mg, 0.3 mmol), compound **10b** was obtained as a brown oil (83 % yield). ¹H NMR (300 MHz, CDCl₃): δ 5.78 (m, 1H, CH=CH), 5.66 (m, 1H, CH=CH), 5.02 (m, 1H, CHOH), 2.96 (m, 1H, A part of ABXX' system NCHH'), 2.88 (m, 1H, NCH), 2.58 (m, 1H, B part of ABXX' system NCHH'), 2.44 (s, 3H, NMe), 2.28 (m, 1H, A part of ABXX' system CH₂CHH'), 2.10-2.04 (m, 2H, B part of ABXX' systems CH₂CHH' and A part of ABXX' system CH(OH)CHH'), 2.02 (s, 3H, COCH₃), 1.63 (m, 1H, B part of ABXX' system CH(OH)CHH'), 1.53 (m, 2H, CH₂), 1.23 (m, 34H, 17 x CH₂), 0.86 (t, *J* = 6.0 Hz, 3H, CH₃). ¹³C NMR (75 MHz, CDCl₃): δ 171.15 (CO), 127.47 (CH=CH), 125.17 (CH=CH), 71.37 (CHOH), 58.65 (NCH), 50.24 (NCH₂), 42.30 (NMe), 37.69 (CH₂), 35.47 (CH₂), 32.22 (CH₂), 29.99-29.85-29.78-29.74-29.66 (15 x CH₂), 25.50 (CH₂), 23.81 (CH₂), 21.53 (COCH₃), 14.25 (CH₃). HRMS (ESI) calcd for C₂₉H₅₆NO₂, [M+H]⁺ 450.4311, found 450.4324.

4.1.7.3 (*R*)-1-((*R*)-1-methyl-1,2,5,6-tetrahydropyridin-2-yl)henicosan-2-yl acetate (**10c**).

Following the general procedure 6 and starting from tetrahydropyridine derivative **6c** (100 mg, 0.26 mmol), compound **10c** was obtained as a brown oil (98 % yield). ¹H NMR (300 MHz, CDCl₃): δ 5.78 (m, 1H, CH=CH), 5.65 (m, 1H, CH=CH), 5.32 (m, 2H, CH=CH), 5.03 (m, 1H, CHOH), 2.90 (m, 1H, A part of ABXX' system NCHH'), 2.75 (m, 1H, NCH), 2.48 (m, 1H, B part of ABXX' system NCHH'), 2.39 (s, 3H, NMe), 2.25 (m, 1H, A part of ABXX' system CH₂CHH'), 2.10-1.85 (m, 9H, 3 x CH₂ and COCH₃), 1.62 (m, 1H, B part of ABXX' system CH(OH)CHH'), 1.53 (m, 2H, CH₂), 1.25 (m, 22H, 11 x CH₂), 0.86 (t, *J* = 6.0 Hz, 3H, CH₃). ¹³C NMR (75 MHz, CDCl₃): δ 171.14 (CO), 130.73 (CH=CH), 130.57 (CH=CH), 128.11 (CH=CH), 125.13 (CH=CH), 71.51 (CHOH), 58.70 (NCH), 50.60 (NCH₂), 42.70 (NMe), 37.82 (CH₂), 35.50 (CH₂), 32.92 (CH₂), 32.21 (CH₂), 30.08-30.00-29.97-29.83-29.80-29.75-29.63-29.50-29.36 (8 x CH₂), 27.52 (CH₂), 25.51 (CH₂), 24.29 (CH₂), 22.99 (CH₂), 21.58 (COCH₃), 14.36 (CH₃). HRMS (ESI) calcd for C₂₇H₅₀NO₂, [M+H]⁺ 420.3842, found 420.3860.

4.1.7.4 (*S*)-1-((*R*)-1-methyl-1,2,5,6-tetrahydropyridin-2-yl)nanodecan-2-yl acetate (**11a**).

Following the general procedure 6 and starting from tetrahydropyridine derivative (**7a**) (118 mg, 0.31 mmol), compound **11a** was obtained as a brown oil (98 % yield). ¹H NMR (300 MHz, CDCl₃): δ 5.74 (m, 1H, CH=CH), 5.54 (m, 1H, CH=CH), 5.03 (m, 1H, CHOH), 2.83 (m, 1H, A part of ABX systems NCHH'), 2.68 (m, 1H, NCH), 2.43 (m, 1H, B part of ABXX' system NCHH'), 2.35 (s, 3H, NMe), 2.06 (m, 2H, CH₂), 2.02 (s, 3H, COCH₃), 1.72 (m, 2H, CH(OH)CH₂), 1.53 (m, 2H, CH(OH)CH₂), 1.24 (m, 28H, 14 x CH₂), 0.87 (t, *J* = 6.3 Hz, 3H, CH₃). ¹³C NMR (75 MHz, CDCl₃): δ 170.84 (CO), 129.60 (CH=CH), 125.20 (CH=CH), 72.66 (CH₂OH), 59.13 (CHN), 49.86 (CH₂N), 42.96 (NMe), 37.94 (CH₂), 34.78 (CH₂), 32.06 (CH₂), 29.83-29.66-29.50 (12 x CH₂), 25.29 (CH₂), 23.76 (CH₂), 22.82 (CH₂), 21.46 (COCH₃), 14.25 (CH₃). HRMS (ESI) calcd for C₂₇H₅₂NO₂, [M+H]⁺ 422.3998, found 422.4015.

4.2. Biology

4.2.1. Cytotoxicity evaluation

4.2.1.1. Cell Culture:

Skin normal fibroblastic cells are purchased from Lonza (Basel, Switzerland), HuH7, Caco-2, MDA-MB-231, HCT116, PC3, MCF7 and NCI-H727 cancer cell lines were obtained from the ECACC collection (Porton Down, UK). Cells are grown at 37°C, 5% CO₂ in ECACC recommended media: DMEM for HuH7, MDA-MB-231 and fibroblast, EMEM for MCF7 and CaCo-2, McCoy's for HCT116 and RPMI for PC3 and NCI-H727. All culture media are supplemented by 10% of FBS, 1% of penicillin-streptomycin and 2 mM glutamine.

4.2.1.2. Cytotoxic assay:

Chemicals are solubilized in DMSO at a concentration of 10 mM (stock solution) and diluted in culture medium to the desired final concentrations. The dose effect cytotoxic assays (IC₅₀ determination) is performed by increasing concentrations of each chemical (final well concentrations: 0.1 μM – 0.3 μM – 0.9 μM – 3 μM – 9 μM - 25 μM). Cells are plated in 96 wells plates (4000 cells/well). Twenty-four hours after seeding, cells are exposed to chemicals. After

48h of treatment, cells are washed in PBS and fixed in cooled 90% ethanol/5% acetic acid for 20 minutes and the nuclei are stained with Hoechst 33342 (B2261 Sigma). Image acquisition and analysis are performed using a Celloomics ArrayScan VTI/HCS Reader (ThermoScientific). The survival percentages are calculated as the percentage of cell number after compound treatment over cell number after DMSO treatment. The relative IC₅₀ are calculated in Microsoft Excel.

4.2.2. Biological assays with MDA-MB-425s cell line

4.2.2.1. Cell Culture:

The human breast cancer cell line MDA-MB-435s was purchased from the American Type Culture Collection (ATCC) and was grown in Alpha-MEM Medium supplemented with 5% Fetal Bovine Serum (FBS). This cell line was transduced with a lentivector containing either an interfering short hairpin RNA (shRNA) specific to SK3 (shSK3 cells) or a nontargeting shRNA (shRD cells) as previously described by Chantôme *et al.*. The Human Embryonic cell line HEK-293 was grown in Dulbecco's modified Eagle's medium supplemented with 5% FBS. These cells were transduced using lentivectors carrying the cDNA of SK3, Orai1 or STIM1 to generate HEK-293 stable expressing cells. Cells were grown at 37 °C in a humidified atmosphere (95% air and 5% CO₂).

4.2.2.2. Transfection assay

2x10⁵ cells/well were seeded with growth medium in a 6-well plate and were transfected with a free-serum opti-MEM medium containing a mixture of Lipofectamine RNAiMax (Invitrogen) and 30 nM of siRNA. Transfected cells were kept incubated at 37°C for 6 hours. The medium was then removed and replaced with a fresh growth medium.

The siRNA sequence directed against Orai1 5'-GCCATAAGACGGACCGACA[dT][dT]-3' as well as the control siRNA sequence 5'-CUGUAUCGAAUGUUAUGAGCC[dT][dT]-3' were purchased from sigma Aldrich.

4.2.2.3. Viability Assay:

Cell viability was determined using the tetrazolium salt reduction method (MTT). Approximately 4 x10⁴ cells were seeded in triplicate in a 24-well plate with different concentrations of the molecules (100 nM, 300 nM, 1 µM, 3 µM and 10 µM) and incubated at 37°C for 24 hours. The medium was then removed, and cells were incubated for 45 min at 37°C with the tetrazolium salt (3-[4,5-dimethylthiazol-2-yl]-2,5-diphenyl tetrazolium bromide). Metabolically active cells (viable cells) reduced the dye into purple formazan. Formazan

crystals were dissolved with DMSO (Dimethylsulfoxide) and the absorbance was measured at 570 nm.

4.2.2.4. Transwell migration assay:

Cell migration was performed using a hollow plastic chamber (Transwell cell culture insert Corning), sealed at one end with an 8µm pore size polyethylene terephthalate membrane and suspended over a larger well. Briefly, 4×10^4 cells were seeded in the upper compartment containing growth medium (5% FBS \pm molecules), and allowed to migrate through the pores to the other side of the membrane. The lower compartment was also filled with growth medium (5% FBS \pm molecules). 24 hours after launching the experiment, non-migrated cells were removed from the topside of the membrane, whereas migrated cells in the bottom side of the inserts were fixed using ice-cold methanol for 10 minutes. Nuclei of migrating cells were stained with DAPI and automatically counted.

4.2.2.5. Intracellular Ca^{2+} measurements

Approximately 1×10^6 Cells were seeded in Petri dishes and loaded with the ratiometric dye Fura2-AM (1µM) for 45 minutes at 37°C. Cells were then collected and centrifuged at 700 x g for 5 minutes. After centrifugation, cells were resuspended in a Ca^{2+} - free solution. 2mM $CaCl_2$ was then injected and Fluorescence emission was measured at 510 nm after an excitation at 340 and 380 nm wavelengths (Hitachi FL-2500).

4.2.3. Electrophysiology

I_{SK3} currents:

Experiments were performed using the whole-cell configuration patch-clamp technique. 2500 cells were seeded into 35 mm Petri dishes. The extracellular solution contained 140mM NaCl, 4mM KCl, 2mM $CaCl_2$, 1mM $MgCl_2$, 10mM HEPES, 0.33 mM NaH_2PO_4 , and 11.5mM D-glucose. The solution was adjusted to pH 7.4 with NaOH. Patch pipettes were pulled to a resistance of 2-4MΩ from borosilicate glass capillary tubes in a two-stage vertical puller (PP-830, Narishige, Tokyo, Japan) and were filled with a pipette solution of 145mM KCl, 1mM $MgCl_2$, 1mM Mg-ATP, 0.7mM $CaCl_2$, 1mM EGTA, and 10mM HEPES. The solution was adjusted to pH 7.2 with KOH. The acute effects of **7a** (2µM) and **10c** (10µM) were tested on HEK-293 SK3⁺ cells using a ramp protocol from -80 mV to +80 mV with a holding potential

of 0 mV (500 ms duration, 4 s intervals) to inactivate endogenous potassium currents. Potassium SK3 currents were analyzed at 0 mV to minimize chloride currents (ECI^- : 0 mV).

I_{CRAC} currents:

HEK293 cells with stable expression of STIM1 and ORAI1 were seeded onto 35 mm round glass coverslips in the 6-well plates 24 h before electrophysiological recordings. Traditional whole-cell patch clamp recordings were performed with an Axopatch 200B and Digidata 1440A (Molecular Devices, San Jose, CA, USA) as previously published^{35, 36}. Pipettes were pulled from borosilicate glass capillaries (World Precision Instruments, Sarasota, FL, USA) with a P-1000 Flaming/Brown micropipette puller (Sutter Instrument Company, Novato, CA, USA) and polished using DMF1000 (World Precision Instruments, Sarasota, FL, USA). Resistances of filled pipettes were 2 to 4 M Ω . Under whole-cell configuration, only cells with tight seals (>16 G Ω) were chosen to perform recordings. 250 ms voltage ramps from +100 to -140 mV were run every 2 seconds for data acquisition. Clampfit 10.3 software was used for data analysis. 8 mM MgCl₂ was included in the pipette solution to inhibit TRPM7 currents.

Bath solution: 115 mM Na-methanesulfonate, 10 mM CsCl, 1.2 mM MgSO₄, 10 mM Hepes, 20 mM CaCl₂, and 10 mM glucose (pH 7.4 with NaOH).

Pipette solution: 135 mM Cs-methanesulfonate, 10 mM EGTA, 8 mM MgCl₂, and 10 mM Hepes (pH 7.2 with CsOH).

4.2.4. Statistical analysis:

All data were expressed as the means for a series of n experiments +/- SEM and analyzed by Mann Whitney test or One-way ANOVA for multiple comparisons using GraphPad Prism 6.0 (San Diego, CA). P-value < 0.05 was considered statistically significant, NS stands for not significant.

Acknowledgements

This work has been developed with technical (ImPACcell platform, Rennes (F) R. Le Guével) and financial supports from the “Réseau Canaux Ioniques” of the “Cancéropôle Grand Ouest”. We are also deeply grateful to the “Ligue contre le Cancer” for financial supports (interregional grants: CSIRGO 2015). This work was supported by “University of Tours”, “Région Centre

Val de Loire”, “INSERM”, and Sana Kouba held her fellowship from the “Ministère de l’enseignement supérieur et de la recherche”.

Supplementary Informations

¹M.J. Berridge, M.D. Bootman, H.L. Roderick. Calcium signalling: dynamics, homeostasis and remodelling. *Nature Reviews. Molecular Cell Biology* 4 (7) (2003) 517-529.

²M. Köhler, B. Hirschberg, C.T. Bond, J.M. Kinzie, N.V. Marrion, J. Maylie, J.P. Adelman. Small-conductance, calcium-activated potassium channels from mammalian brain. *Science*. 273 (1996) 1709-1714.

³S.H. Thompson. Three pharmacologically distinct potassium channels in molluscan neurones. *J. Physiol.* 265 (1977) 465-488.

⁴C.T. Bond, J. Maylie, J.P. Adelman. Small-conductance calcium-activated potassium channels. *Ann N Y Acad. of Sci.* 868 (1999) 370-378.

⁵M.P. Burnham, R. Bychkov, M. Félétou, G.R. Richards, P.M. Vanhoutte, A.H. Weston, G Edwards. Characterization of an apamin-sensitive small-conductance Ca^{2+} -Activated K^{+} channel in porcine coronary artery endothelium: relevance to EDHF. *Br. J. Pharmacol.* 135(5) (2002) 1133-1143.

⁶X-K. Liu, G. Wang, S-D. Chen. Modulation of the activity of dopaminergic neurons by SK Channels: a potential target for the treatment of Parkinson’s disease? *Neuroscience Bulletin*. 26 (2010) 265-271.

⁷K.G. Chandy, E. Fantino, O. Wittekindt, K. Kalman, L-L. Tong, T-H. Ho, G.A. Gutman, M-A. Crocq, R. Ganguli, V. Nimgaonkar, Morris-Rosendahl, J.J. Gargus. Isolation of a novel potassium channel gene HSKCa3 containing a polymorphic CAG repeat: a candidate for schizophrenia and bipolar disorder? *Molecular Psychiatry*. 3 (1998) 32-37.

⁸J.J. Gargus, E. Fantino, G.A. Gutman. A piece in the puzzle: an ion channel candidate gene for schizophrenia. *Mol. Med. Today* 4 (1998) 518-524.

⁹J. Diness, J. Kirchhoff, M. Sheykhzade, T. Jespersen, M. Grunnet. Antiarrhythmic effect of either negative modulation or blockade of small conductance Ca^{2+} -activated K^{+} channels on

ventricular fibrillation in guinea pig Langendorff-perfused heart, *J. Cardiovasc. Pharmacology* 66 (2015) 294-299.

¹⁰ X.Y. Qi, J.G. Diness, B.J. Brundel, X.B. Zhou, P. Naud, C.T. Wu, H. Huang, M. Harada, M. Aflaki, D. Dobrev, M. Grunnet, S. Nattel. Role of small-conductance calcium-activated potassium channels in atrial electrophysiology and fibrillation in the Dog. *Circulation* 129 (2014) 430-440.

¹¹ L. Skibsbjerg, C. Poulet, J.G. Diness, B.H. Bentzen, L. Yuan, U. Kappert, K. Matschke, E. Wettwer, U. Ravens, M. Grunnet, T. Christ, T. Jespersen. Small-conductance calcium-activated Potassium (SK) channels contribute to action potential repolarization in human atria. *Cardiovasc. Res.* 103 (2014) 156-167.

¹² M.S. Taylor, A.D. Bonev, T.P. Gross, D.M. Eckman, J.E. Brayden, C.T. Bond, J. P. Adelman, M.T. Nelson. Altered expression of small-conductance Ca^{2+} -activated K^{+} (SK3) channels modulates arterial tone and blood pressure. *Circulation Research* 93 (2003) 124-131.

¹³ M. Potier, V. Joulin, S. Roger, P. Besson, M-L. Jourdan, J-Y. LeGuennec, P. Bournoux, C. Vandier. Identification of SK3 channel as a new mediator of breast cancer cell migration », *Mol. Cancer Ther.* 5 (2006) 2946-2953.

¹⁴ A. Chantôme, M. Potier-Cartereau, L. Clarysse, G. Fromont, S. Marionneau-Lambot, M. Guéguinou, J-C. Pagès, C. Collin, T. Oullier, A. Girault, F. Arbion, J-P. Haelters, P-A. Jaffrès, M. Pinault, P. Besson, V. Joulin, P. Bournoux, C. Vandier. Pivotal role of the lipid raft SK3-Orai1 complex in human cancer cell migration and bone metastases. *Cancer Res.* 73 (2013) 4852-4861.

¹⁵ I.J. Diel. Bisphosphonates in breast cancer patients with bone metastases. *Breast Care* 5, (2010) 306-311.

¹⁶ J.P. Vincent, H. Schweitz, M. Lazdunski. Structure-function relationships and site of action of apamin, a neurotoxic polypeptide of bee venom with an action on the central nervous system. *Biochemistry* 14 (1975) 2521-2525.

¹⁷ V. Quintero-Hernández, J.M. Jiménez-Vargas, G.B. Gurrola, H.H.F. Valdivia, L.D. Possani. Scorpion venom components that affect ion-channels function. *Toxicon* 76 (2013) 328-342.

¹⁸ P.T.J. Tan, S. Ranganathan, V. Brusic. Deduction of functional peptide motifs in scorpion toxins. *J. Peptide Sci.* 12 (2006) 420-427.

¹⁹ M. Hugues, G. Romey, D. Duval, J.P. Vincent, M. Lazdunski. Apamin as a selective blocker of the calcium-dependent potassium channel in neuroblastoma cells: voltage-clamp and biochemical characterization of the toxin receptor. *Proc. Natl. Acad. Sciences U.S.A.* 79 (1982) 1308-1212.

-
- ²⁰ a) M.A. Schumacher, A.F. Rivard, H.P. Bächinger, J.P. Adelman. Structure of the gating domain of a Ca^{2+} -activated K^+ channel complexed with Ca^{2+} /calmodulin. *Nature*. 410 (2001) 1120-1124; b) L.T.-Y. Cho, A.J. Alexandrou, R. Torella, J. Knafels, J. Hobbs, T. Taylor, A. Loucif, A. Konopacka, S. Bell, E. B. Stevens, J. Pandit, R. Horst, J.M. Withka, D.C. Pryde, S. Liu, G.T. Young. An intracellular allosteric modulator binding pocket in SK2 ion channels is shared by multiple chemotypes. *Structure*. 26 (2018) 1–12.
- ²¹ S. Dilly, A. Graulich, A. Farce, V. Seutin, J.-F. Liégeois, P. Chavatte. Identification of a pharmacophore of SKCa channel blockers, *Journal of Enzyme Inhibition and Medicinal Chemistry*. 20 (2005) 517-523.
- ²² P. M. Dunn. Dequalinium, a selective blocker of the slow after hyperpolarization in rat sympathetic neurones in culture. *Eur. J. Pharmacol.* 252 (1994) 189-194. b) D. Galanakis, C. A. Davis, B. Del Rey Herrero, C.R. Ganellin, P.M. Dunn, D.H. Jenkinson. Synthesis and structure-activity relationships of dequalinium analogues as K^+ channel blockers. Investigations on the role of the charged heterocycle. *J. Med. Chem.* 38 (1995) 595-606.
- ²³ J. Campos Rosa, D. Galanakis, C. Robin Ganellin, P.M. Dunn, D.H. Jenkinson. Bis-quinolinium cyclophanes : 6,10-diaza-3(1,3),8(1,4)-dibenzene-1,5(1,4)-diquinolinacyclodecaphane (UCL 1684), the first nanomolar, non-peptidic blocker of the apamin-sensitive Ca^{2+} -activated K^+ channel. *J. Med. Chem.* 41 (1998) 2-5.
- ²⁴ D. Yang, L. Arifhodzic, C. Robin Ganellin, D.H. Jenkinson. Further studies on bis-charged tetraazacyclophanes as potent inhibitors of small conductance Ca^{2+} -activated K^+ channels, *Eur. J. Med. Chem.* 63 (2013) 907-923; b) J-Q. Chen, D. Galanakis, C. Robin Ganellin, P. M. Dunn, D. H. Jenkinson. Bis-quinolinium cyclophanes: 8,14-Diaza-1,7(1,4)-diquinolinacyclotetradecaphane (UCL 1848), a highly potent and selective, nonpeptidic blocker of the apamin-sensitive Ca^{2+} -activated K^+ channel. *J. Med. Chem.* 43 (2000) 3478-3481.
- ²⁵ A. Graulich, S. Dilly, A. Farce, J. Scuvé-Moreau, O. Waroux, C. Lamy, P. Chavatte, V. Seutin, J.F. Liégeois. Synthesis and radioligand binding studies of bis-isoquinolinium derivatives as small conductance Ca^{2+} -activated K^+ channel blockers. *J. Med. Chem.* 50 (2007) 5070-5075.
- ²⁶ J-F. Liégeois, J. Wouters, V. Seutin, S. Dilly. Bis-(1,2,3,4-tetrahydroisoquinolinium): A chiral scaffold for developing high-affinity ligands for SK channels, *ChemMedChem* 9 (2014) 737-740.
- ²⁷ C. Hougaard, B.L. Eriksen, S. Jørgensen, T.H. Johansen, T. Dyhring, L.S. Madsen, D. Strøbæk, P. Christophersen. Selective positive modulation of the SK3 and SK2 subtypes of small conductance Ca^{2+} -activated K^+ channels. *Br. J. Pharmacol.* 151 (2007) 655-665.

-
- ²⁸ N. Coleman, B.M. Brown, A. Oliván-Viguera, V. Singh, M.M. Olmstead, M.S. Valero, R. Köhler, H. Wulff. New positive Ca^{2+} -activated K^+ channel gating modulators with selectivity for $\text{K}_{\text{Ca}3.1}$. *Mol Pharmacol* 86 (2014) 342-357.
- ²⁹ a) U.S. Sørensen, D. Strøbæk, P. Christophersen, C. Hougaard, M.L. Jensen, E. Ø. Nielsen, D. Peters, L. Teuber. Synthesis and structure-activity relationship studies of 2-(*N*-substituted)-aminobenzimidazoles as potent negative gating modulators of small conductance Ca^{2+} -activated K^+ channels. *J. Med. Chem.* 51 (2008) 7625-7634; b) D.P.Jenkins, D. Strøbæk, C. Hougaard, M L. Jensen, R. Hummel, U.S. Sørensen, P. Christophersen, H. Wulff. Negative gating modulation by (R)-*N*-(benzimidazol-2-yl)-1,2,3,4-tetrahydro-1-naphthylamine (NS8593) depends on residues in the inner pore vestibule: pharmacological evidence of deep-pore gating of $\text{K}_{\text{Ca}2}$ channels. *Mol. Pharmacol.* 79 (2011) 899-909.
- ³⁰ M. Potier, A. Chantôme, V. Joulin, A. Girault, S. Roger, P. Besson, M-L Jourdan, J-Y LeGuennec, P. Bougnoux, C. Vandier. The SK3/ $\text{KCa}2.3$ potassium channel is a new cellular target for edelfosine. *Br. J. Pharmacol.* 162 (2011) 464-479.
- ³¹ A. Girault, J.-P. Haelters, M. Potier, A. Chantôme, M. Pinault, S. Marionneau-Lambot, T. Oullier, G. Simon, H. Couthon-Gourvès, P.-A. Jaffrès, B. Corbel, P. Bougnoux, V. Joulin, C. Vandier. New alkyl-lipid blockers of SK3 channels reduce cancer cell migration and occurrence of metastasis. *Curr. Cancer Drug Targets* 11 (2011) 1111-1125.
- ³² P-A. Jaffrès, C. Gajate, A.M. Bouchet, H. Couthon-Gourvès, A. Chantôme, M. Potier-Cartereau, P. Besson, P. Bougnoux, F. Mollinedo, C. Vandier. Alkyl ether lipids, ion channels and lipid raft reorganization in cancer therapy. *Pharmacology & Therapeutics* 165 (2016) 114-131.
- ³³ A. Boussonnière, T. Ranaivondrambola, J. Lebreton, M. Mathé-Allainmat. A rapid access to (\pm)-sedamine and some original *N*-benzyl unsaturated analogues. *Synthesis* 14 (2010) 2456-2462.
- ³⁴ Notes: As we earlier observed (ref. 33) isomerisation at the C2 position of the tetrahydropyridine could be observed in the presence of a catalytic amount of Pd/C. In the same study we have published the RX data of the 3,4-unsaturated analog of (\pm)-sedamine obtained following the same procedure and so confirmed the *syn*-diastereoselectivity of the reduction step with $\text{NaBH}(\text{OAc})_3$.
- ³⁵ X. Zhang, T. Pathak, R. Yoast, S. Emrich, P. Xin, R.M. Nwokonko, M. Johnson, S. Wu, S. Delierneux, M. Gueguinou, N. Hempel, J.W. Putney, D. Gill, M. Trebak. A calcium/cAMP signaling loop at the ORAI1 mouth drives channel inactivation to shape NFAT induction. *Nature Communications*. 10 (2019) 1971.

³⁶ X. Zhang, W. Zhang, J.C. Gonzalez-Cobos, I. Jardin, C. Romanin, K. Matrougui, M. Trebak. Complex role of STIM1 in the activation of store-independent Orai1/3 channels. *Journal of General Physiology*. 143 (2014) 345-359.